The fall of charged particles under gravity: A study of experimental problems

T. W. Darling, F. Rossi, G. I. Opat, and G. F. Moorhead

School of Physics, University of Melbourne, Parkville, Victoria 3052, Australia

There are currently proposals to test the weak equivalence principle for antimatter by studying the motion of antiprotons, negative hydrogen ions, positrons, and electrons under gravity. The motions of such charged particles are affected by residual gas, radiation, and electric and magnetic fields, as well as gravity. The electric fields are particularly sensitive to the state of the "shielding" container. This paper reviews, and extends where necessary, the physics of these extraneous influences on the motion of charged particles under gravity. The effects considered include residual gas scattering; wall potentials due to patches, stress, thermal gradients, and contamination states; and image-charge-induced dissipation.

CONTENTS

ABBREVIATIONS USED IN TEXT

DMRT: Dessler *et al.*, 1968.
LWF: Lockhart, Witteborn, and Fairbank, 1977.
SB: Schiff and Barnhill, 1966.
TOF: Time of flight.
WF: Witteborn and Fairbank, 1967.

I. INTRODUCTION

The gravitational properties of antimatter have been a topic of theoretical speculation for over 30 years, and yet direct experimental tests have never been performed. At present, Galilean free-fall experiments are being developed to compare the acceleration of antiprotons and H⁻ ions in the Earth's gravity (Beverini *et al.*, 1986; Goldman *et al.*, 1987). Other experiments have already investigated the fall of electrons (Witteborn and Fairbank, 1967) and may be extended to positrons in the future (Henderson and Fairbank, 1984). Such experiments test the weak equivalence principle for antimatter, which asserts that in a given gravitational field all test particles of the same initial velocity fall with the same acceleration (Ohanian, 1977).

Newton was the first to recognize the distinction between inertial mass, passive gravitational mass, and active gravitational mass (for a review, see Bondi, 1957). Inertial mass m_I is the quantity that enters Newton's second law: $F = m_I a$, where a is the acceleration. Passive gravitational mass m_{GP} is the mass on which the gravitational field acts: $F = m_{GP} g$, where g is the gravitational field. Active gravitational mass m_{GA} is the mass that is the source of gravitational fields and hence is the mass that enters Poisson's equation. In Newtonian physics, the third law implies the equality of active and passive gravitational masses, $m_{GP} = m_{GA} = m_G$, and we refer simply to the gravitational mass. For a body falling in a gravitational field, $F = m_I a = m_G g$, so that its acceleration is given by $a = (m_G / m_I) g$. For bodies made of normal matter, it is an empirical fact, and the basis of the weak equivalence principle, that the inertial mass and the gravitational mass are equal, $m_G = m_I = m$; hence $a = g$.

To explain the observed abundance of normal matter over antimatter in our neighborhood of the universe, Morrison and Gold (1957; see also Morrison, 1958) proposed that antimatter may have negative gravitational mass. Thus antimatter would be repelled by the gravitational field of normal matter, e.g., rising in the Earth's field. However, this notion, sometimes referred to as "antigravity," violates the weak equivalence principle.

For normal matter, the weak equivalence principle has been verified with high accuracy in several well-known classic experiments, such as those of von Eötvös *et al.* (1922); Roll, Krotkov, and Dicke (1964); Braginsky and Panov (1971; Will, 1984, reviews the status up to 1984; and most recently by Adelberger *et al.* (1990). Schiff (1958) argued that the results of the von Eötvös experiments indirectly disproved "antigravity" for positrons. Virtual positrons in the Coulomb field in atoms of normal matter contribute to the gravitational mass of those

237

atoms and, by his estimates, would have produced measurable effects were they to have negative gravitational mass. However, in Morrison and Gold's proposal, only real stable antimatter experiences "antigravity," while the electromagnetic mass contribution considered by Schiff is normally attracted. Good (1961) argued that the existence of the long-lived neutral K meson, a coherent linear combination of the K^0 and anti-K^0, and the absence of its decay into two pions, established the equality of the gravitational masses of the K^0 and anti-K^0 to very high accuracy. However, Goldman and Nieto (1982; see also Beverini *et al.*, 1986) have pointed out the assumptions, limitations, and indirectness of Schiff's, Good's, and other such arguments.

The original motivation for "antigravity" faded in the late 1970's as several authors realized that, under certain conditions, the new grand unified theories could allow a baryon asymmetry to evolve during the early history of the universe, thereby explaining the absence of antimatter (see Kolb and Turner, 1983, for a review of baryogenesis). Despite this, anomalous gravitational properties of antimatter were still being considered by some authors—Scherk (1979), Goldman and Nieto (1982), and Macrae and Riegert (1984)—who were working on quantum gravity theories based on local supersymmetry. Such theories predict the existence of a spin-1 graviphoton and a spin-0 graviscalar, partners to the conventional spin-2 graviton, which acquire small masses from symmetry breaking (Goldman *et al.*, 1986). These produce additional finite-range Yukawa-potential interactions, distinguishable from normal inverse-square-law gravity by their composition dependence, i.e., violation of the weak equivalence principle. Experimental evidence cited in support of this was the claimed deviation from Newton's inverse square law in analyses of geophysical measurements (Stacey *et al.*, 1987). Quite unlike the early notion of "antigravity," such interactions are expected to produce a slightly larger downward acceleration for antiparticles in the Earth's gravity than for their counterparts. Goldman *et al.* (1987) estimate that antiprotons may fall a few percent faster than protons.

On a separate front, the controversial reanalysis by Fischbach *et al.* (1986) of the original von Eötvös experiments provided slight evidence for a violation of the weak equivalence principle, suggesting the presence of a "fifth force." Some of the subsequent weak equivalence principle tests (Boynton *et al.*, 1987; Thieberger, 1987) found supporting evidence. Deviations from Newton's inverse square law were also reported in tower gravity measurements (Eckhardt *et al.*, 1988). Goldman *et al.* (1987) and Nieto *et al.* (1988) pointed out that such phenomena may be simply explained in terms of the quantum gravity theories. However, many more experiments have failed to find such evidence; recently, the most stringent bounds were set by Adelberger *et al.* (1990).

In spite of all this activity, the acceleration of antimatter in a gravitational field has never been directly measured. The first efforts in this direction began in the

mid 1960s by a group at Stanford University, under the leadership of W. M. Fairbank, with an ingenious series of experiments aiming ultimately to measure the acceleration of positrons in the Earth's gravitational field. To date, only precursory experiments have been carried out on electrons. A separate initiative, begun in the early 1980s by T. Goldman and M. M. Nieto of Los Alamos National Laboratory, now a large international consortium (Beverini *et al.*, 1986), is currently developing a similar experiment, using the LEAR facilities at CERN, to compare the acceleration of H^- ions and antiprotons. Adelberger *et al.* (1990) have argued that weak equivalence principle tests already constrain any difference in the acceleration of protons and antiprotons to well below the one-percent level of accuracy expected of this experiment; however, such an indirect argument rests on a preconceived theoretical framework (Nieto and Goldman, 1991). Quite independently of any theoretical motivation or speculation, such experiment should be performed. The sheer paucity of fundamental tests of gravity makes any new experiment worthwhile, whatever the final result.

Both the Stanford and the CERN experiments face extreme difficulties, since the electron, positron, H^- ion, and antiproton carry electric charge. The comparative weakness of the gravitational interaction with the electromagnetic interaction demands that these particles be isolated from electromagnetic fields. We note that the force of attraction of an electron to the Earth is balanced by the repulsion of another electron located 5 meters distant. Antiprotons and H^- ions are less sensitive to electric fields than electrons by the ratio of their masses, but even so require careful shielding.

Witteborn's pioneering work at Stanford (1965) appeared to demonstrate that free electrons could be satisfactorily shielded from most extraneous fields by enclosing them in an evacuated vertical copper drift tube cooled to 4.2 K. Measurements of the vertical time of flight determined the net force on the electrons (Witteborn and Fairbank, 1967). The antiproton experiment derives much from the Stanford technique. However, the Witteborn-Fairbank measurement (henceforth referred to as WF) has been the subject of some controversy, since theoretical expectations of the electric fields induced by the effects of gravity on the drift tube, and due to patch potential variations on its surface, appear to preclude such a measurement. We shall discuss these problems in subsequent sections.

Since the interpretation of the results for antimatter are of fundamental importance, we have reviewed (see, in particular, Witteborn and Fairbank, 1977 and Beverini *et al.*, 1986) and extended where necessary the analysis of the forces experienced by a charged particle in a drift tube.

II. DRIFT-TUBE EXPERIMENTS

In this section we review the Stanford and Los Alamos/CERN drift-tube experiments, as an orientation
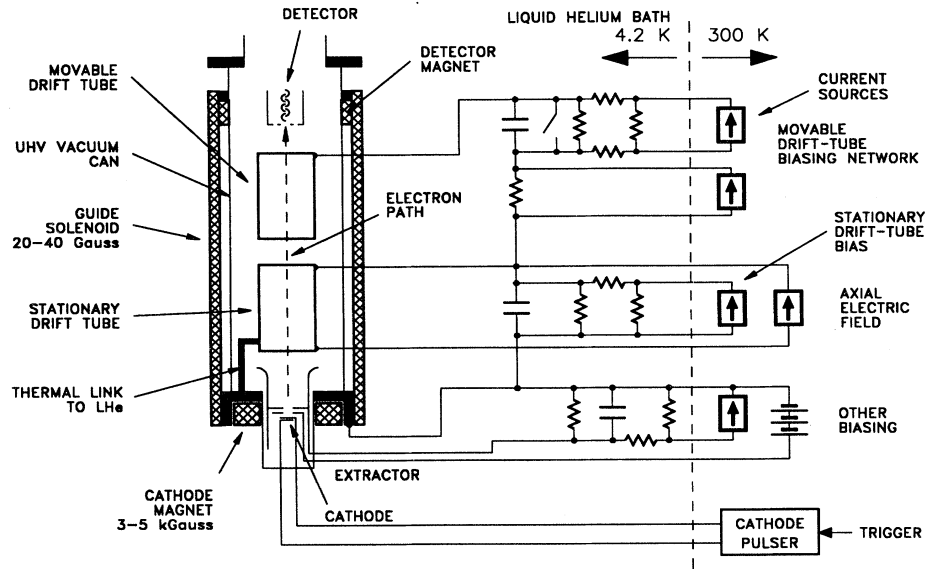
FIG. 1. Drift-tube apparatus used by the Stanford group in their free-fall experiments with electrons. Not shown is a second movable drift tube, located above the stationary drift tube. The second drift tube was used in an alternative technique, but was not as successful as the single-drift-tube method (Fairbank *et al.*, 1974). Normally it was electrically biased so as to have no significant effect on the time of flight of electrons, and it is ignored in this review. Reproduced from Lockhart (1976).

for the sections that follow.

We begin by describing the Stanford drift-tube apparatus used to measure the gravitational acceleration of free electrons (Fig. 1); many of the principles involved have been adapted to the Los Alamos/CERN apparatus. Figure 1 corresponds to the version used by Lockhart *et al.* (1977); other than changes to the drift-tube bias circuits, it is the same as that used by Witteborn and Fairbank (1967). A detailed account of the design and operation of the apparatus may be found in Witteborn and Fairbank (1977); here we give a brief summary.

Short bursts of about 10^9 electrons with a distribution of energies are emitted upwards from a cold cathode, through the drift tube, and detected at the top by a windowless electron multiplier. An axial guide magnetic field constrains them to move along the axis of the metal drift tube. The electrical potential of the drift tube with respect to the rest of the apparatus is adjusted so that the electrons near the peak of the energy distribution move slowly only while inside the drift tube. Outside they move very fast, so that the time necessary to reach the top of the apparatus is negligibly different from their time of flight through the drift tube. The height of the drift tube was $H = 91$ cm, with a radius $R = 2.5$ cm.

Electrons entering the drift tube must have a minimum critical velocity v_c to reach the top of the tube and be detected. If they experience only a uniform downward acceleration a, over the length of the drift tube, H, then

$$v_c = \sqrt{2Ha} \quad . \tag{2.1}$$

Ideally, the distribution of flight times will show a clean cutoff

$$t_c = \sqrt{2H/a} \quad . \tag{2.2}$$

Thus, if gravity is the only force acting on the electrons, their acceleration could be determined from measurements of t_c and H. Normally, one would expect $a = g$, in which case $v_c = 4.22$ m/s and $t_c = 0.43$ s (Fig. 2). Equations (2.1) and (2.2) apply to any particle. Thus in both the electron and the antiproton experiments, the determination of the gravitational acceleration involves particle speeds just under 10 m/s, with flight times just under 1 s, for drift tubes 1–2 meters high.

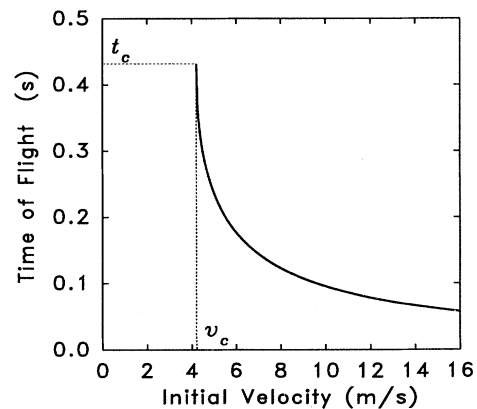Clearly, low-energy electrons of order $mgH \approx 10^{-10}$ eV

FIG. 2. Time of flight plotted against the initial vertical velocity on entering the drift tube in an ideal experiment, for $H = 0.91$ m and $a = 9.8$ m/s^2. The cutoff time is t_c, and v_c is the corresponding critical minimum velocity necessary to reach the top.

are most sensitive to gravity. While the total number of electrons emitted in each pulse is quite large, most have much higher energies. Moreover, to reduce sensitivity to magnetic-field variations, only electrons in the magnetic ground state are used. A high-field magnet surrounding the cathode is employed to spatially segregate those in the ground state from the others, which are accelerated quickly through the system. As a result, there is typically one useful low-energy electron per pulse, requiring a large number of pulses to accumulate a satisfactory time-of-flight (TOF) distribution.

In practice, WF fitted a five-parameter nonlinear model to the observed TOF distributions to account for a number of obfuscating effects:

(a) Background electron counting noise limits the precision with which t_c can be visually determined; one of the fit parameters is the constant noise background.

(b) Two parameters account for the energy distribution of the electrons as they enter the tube. One is related to the total number of electrons launched. The other accounts for cooling of the electrons as the initial cloud emitted by the cathode interacts via the Coulomb force, considerably enhancing the number of slow electrons.

(c) Another parameter accounts for delayed emission of electrons from potential traps along the flight path.

(d) The finite length of the drift tube allows some penetration of external fields, so that the effectively shielded length of the tube is slightly smaller than its physical length. Near the ends of the tube, the potential experienced by the electrons was approximated using the known bias voltages and geometry of the apparatus.

(e) The fifth parameter is the desired constant force experienced by the electrons in the effectively shielded portion of the drift tube.

An additional feature is the use of axial electric fields, produced by passing electric currents through the walls of the drift tube, to apply known forces to the electrons. As shown in Fig. 3, this enables calibration and verification of the proper operation of the apparatus and analysis procedures, as well as improving accuracy. The ambient force (ideally only gravity) is determined from the zero applied field intercept in Fig. 3.

The great challenge of this experiment is to eliminate all nongravitational forces acting on the electron. Ambient electric fields are the most problematic, since the force of gravity on electrons is only -5.6×10^{-11} eV/m; thus electric fields must be reduced well below 10^{-11} V/m. The purpose of the metal drift tube is to act as an electrostatic shield; however, unlike textbook shields, real metallic shields are not generally electrostatic equipotentials, due to contact potential phenomena. The electrostatic potential just outside any two metal surfaces that are in thermodynamic equilibrium will differ by an amount, referred to as the contact potential difference, given by the difference of their work functions. Work-function variations may arise on the surface of a drift tube due to inequivalent crystal facets or regions of con-
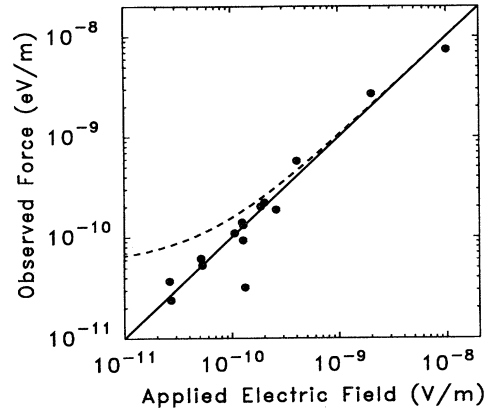

FIG. 3. Measured force vs applied electric field in the WF experiment, determined from their five-parameter analysis of time-of-flight distributions. Applied fields of both signs were used; the plot shows only the absolute values. The solid line shows the electrostatic force expected for electrons, without gravity or any other ambient force. The dashed line shows the expected behavior when gravity is the only ambient force. A straight-line fit to the measured points yields the zero applied field intercept and hence the ambient force. Their null result was the average of 11 data sets using applied fields with magnitudes less than 2.5×10^{-10} V/m. Reproduced from the published data of Witteborn and Fairbank (1967).

tamination; this is known as the patch effect (Herring and Nichols, 1949). Typically, observed surface-potential variations range from 0.01–0.1 V. Even for a perfectly uniform surface, additional gravity-induced electric fields are expected. In essence, these arise because gravity redistributes the electrons and ions in the drift-tube walls. These effects will be discussed in detail in Secs. V and VI.

Clearly, the composition of the drift tube's surface is of great importance. Made of electroformed OFHC copper, the drift tube was required to have very uniform interior dimensions and an amorphous surface to reduce the size of patches and hence the magnitude of axial patch fields (see Sec. V). Extended exposure to air allowed a surface layer of contaminants, 20–50 Å thick, to form, including oxide, traces of carbon, sulphur, and chlorine (Hanni and Madey, 1978); other oxidation data, though, would suggest a layer at least 100–200 Å thick (Cabrera and Mott, 1949). Surface texture variations were present with crystallite sizes below 1 μm. The drift tube was baked to 100 °C in vacuum, driving off adsorbed water vapor; however, most of the contaminant layer would have remained, since much higher temperatures and ion bombardment are required to produce an atomically clean surface (Delchar, 1971). Although the underlying copper is polycrystalline, the relatively large thickness (compared to interatomic dimensions) and complex chemistry of the contaminant layer would make the surface nearly amorphous, as intended.

The Stanford group were well aware of the limitations imposed by patch fields, axial potential variations of order 10^{-6} V were expected, producing forces 10^4 larger

than gravity. However, in a feasibility experiment, Witteborn (1965) found that he could measure electrons with energies as low as 10^{-11} eV, suggesting that the patch effect was not present, possibly due to masking by the preferential adsorption of contaminants on the drift-tube surface.

Before WF, Schiff and Barnhill (1966) calculated the vertical gravity-induced electric field in the drift tube to be $\mathbf{E}_{SB} = -(mg/e)\hat{z}$ (henceforth referred to as the SB field), where $\hat{z}$ is a unit vector in the upward direction. Such a field is expected to be generated within the drift-tube walls to balance the force of gravity on the electrons in the walls; consequently, it should also exactly cancel the force of gravity on free electrons traveling along the drift-tube axis. We note that the mass that enters the Schiff-Barnhill equation is in fact the gravitational mass of electrons $m_G(e^-)$, and that in the ideal case where all other forces are negligible, a null force result would always be obtained for electrons even if, for some reason, electrons did not obey the equivalence principle. Measurements on a positron are expected to yield a nonzero acceleration, since, in the above ideal case, the net force would be $-[m_G(e^-)+m_G(e^+)]g\hat{z}$. Thus only the sum of the electron's and positron's gravitational masses can be determined. Assuming both particles obey the equivalence principle, the positron would fall with acceleration $2g$. The WF result was that electrons in their drift tube had an acceleration of $0\pm0.09g$ (Fig. 3), perfectly consistent with the presence of the SB field and the absence of the patch effect. As noted by them, this result proves only that the force of gravity on electrons in the wall of the drift tube is the same as that on free electrons on the axis.

However, soon after, Dessler *et al.* (1968, henceforth referred to as DMRT) published their calculation of the gravity-induced electric field, finding in addition to the SB field an upward field $\mathbf{E}_{DMRT} = \gamma(Mg/e)\hat{z}$ (the DMRT field), where M is the atomic mass (of Cu in this case) and γ is a constant of order 0.1. This field arises from the differential compression of the drift tube as it supports its own weight. Since $M/m \approx 10^5$, the DMRT field should have overwhelmed gravity and the SB field in the WF experiment. Herring (1968) reconciled the two calculations, and it is now generally agreed (Schiff, 1970) that the DMRT calculation is essentially correct. It would seem then that either the DMRT and patch fields were being simultaneously masked or shielded, or something was amiss in the experiment. In the former case, the shielding effect must be very selective, since the SB field and fields produced by running electric currents up the tube were not shielded.

Suspecting that the low temperature (4.2 K) used in the WF experiment might be responsible in some way for the absence of the large fields, Lockhart, Witteborn, and Fairbank (1977, henceforth referred to as LWF) repeated the experiment at temperatures ranging from 4.2 to 300 K, finding a sharp transition in the force on electrons at 4.5 K (Fig. 4). At 4.2 K the results were consistent with
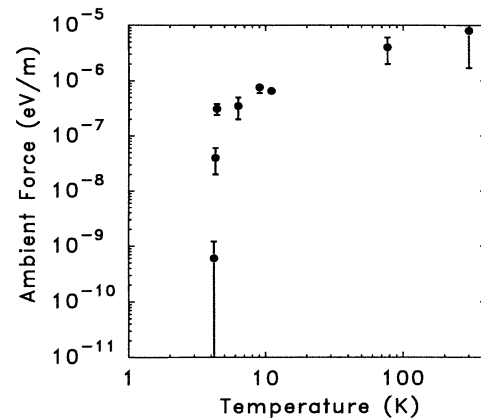

FIG. 4. Temperature dependence of the ambient force on electrons in the drift tube, showing evidence for a temperature-dependent shielding effect. Reproduced from the published data of Lockhart, Witteborn, and Fairbank (1977).

WF, but above 4.5 K the force was consistent with the estimates for the patch and DMRT fields. Thus the success of the 1967 experiment was attributed to a fortuitous and selective temperature-dependent shielding effect.

Various theoretical proposals have been unable to predict a shielding effect with a 4.5-K transition temperature (Schiff, 1970; Trammell and Rorschach, 1970; Hanni and Madey, 1978; Hutson, 1978; Bardeen, 1982). Independent experiments (Free *et al.*, 1979; Rzchowski *et al.*, 1987), including those conducted in our group (Darling, 1989 and Rossi, 1991, which will be the subjects of future papers), have not revealed such a shielding effect. Recently, however, the original 1977 data has been partially retracted (Lockhart *et al.*, 1991). This aspect of the drift-tube experiments remains somewhat controversial, since the unambiguous interpretation of future results for positrons and antiprotons relies on this effect.

The positron version of the experiment has not been completed due to the difficulties in obtaining a suitable source of slow positrons. Fairbank *et al.* (1974) and Henderson and Fairbank (1984) discuss these efforts.

The antiproton drift-tube experiment, to be conducted at CERN, has not yet reached the operational stage; the reader is referred to the extensive review by Beverini *et al.* (1986; see also Brown *et al.*, 1990). In essence, five MeV antiprotons from LEAR are to be cooled in a number of stages to temperatures ranging from 4 to 10 K, held in a launching trap, and then released into the drift tube, approximately 100 at a time. One option being considered is to launch the particles downwards instead of upwards. The force of gravity on antiprotons is -1.0×10^{-7} eV/m. Of the 100 launched, only one is expected to be in the useful low-energy range ($<10^{-6}$ eV) that is sensitive to gravity. A significant advantage of this experiment is that antiprotons are less sensitive to ambient electric fields than electrons by a factor of 1836, the ratio of their masses. Even so, if the DMRT and patch fields are present as predicted, the resulting force

would still be comparable to or exceed gravity. However, only a differential measurement between antiprotons and H^- is proposed. These ions provide a calibration standard, with almost identical electromagnetic properties to antiprotons, which may be used to map out and correct for electromagnetic field effects within the drift tube. Preliminary measurements are proposed with heavier ions, which may help to verify and elucidate the shielding effect claimed by the Stanford group.

Table I summarizes some important characteristics of the two drift-tube experiments. In the following sections we examine the interactions experienced by charged particles in such apparatus.

III. INTERACTIONS OF A CHARGED PARTICLE

A charged particle is coupled to its environment by

(a) the gravitational field through its mass m,
(b) the electric field through its charge q,
(c) electric-field gradients through its polarizability α_e,
(d) the magnetic field through its charge and velocity $\mathbf{v}$,
(e) magnetic-field gradients through its magnetic moment μ and diamagnetic polarizability α_m,
(f) radiation through the photon cross section, σ_r, and
(g) residual gas scattering through the cross section, σ_g.

We believe that (a)–(g) exhaustively lists all the "han-

dles" by which charged particles are coupled to the external world. In the rest of this and subsequent sections, we shall investigate each of these couplings in turn.

A. Gravitational

The term "gravitational" in the above list refers to nonelectromagnetic interactions of adequate range. In the absence of nonstandard phenomena, the gravitational force on a nonrelativistic particle is given by

$$\mathbf{F}_g = m\mathbf{g} \ , \tag{3.1}$$

where $\mathbf{g}$ is the gravitational field. In terms of the gravitational potential ψ, $\mathbf{g}$ is given by

$$\mathbf{g} = -\nabla\psi$$
$$= -g\hat{\mathbf{z}} \ . \tag{3.2}$$

B. Electrical

Unwanted electrical interactions are by far the most serious problem in free-falling charge experiments. The magnitude of the electric field that just balances gravity is given by

$$E = mg/e$$
$$= \begin{cases} 0.56\times10^{-10} \text{ V/m} & \text{(electrons)} \\ 1.02\times10^{-7} \text{ V/m} & \text{(protons)} \end{cases} \ . \tag{3.3}$$

TABLE I. Characteristics of the drift-tube experiments.

Experimental parameter	Stanford experiments (electrons)	Los Alamos/CERN Experiments (antiprotons/H^-)
Status	Electron experiments completed; positron experiment under review	Under development
Gravitational force, $-mg$	-0.56×10^{-10} eV/m	-1.02×10^{-7} eV/m
Drift-tube height, H	0.91 m	1–2 m
Drift-tube radius, R	2.5 cm	1–2 cm
Drift-tube composition	Polycrystalline-oxidized copper	Bronze, various surface coatings under review
Critical speed, $v_c(H=1$ m, $a=9.8$ m/s^2)	4.43 m/s	4.43 m/s
TOF cutoff time, $t_c(H=1$ m, $a=9.8$ m/s^2)	0.45 s	0..45 s
Axial magnetic guide field, B_z	20–40 G	10–50 kG
Cathode magnetic field	3–5 kG	Not used
Particle source	Cold cathode	LEAR, deceleration and cooling stages
Number of particles launched per pulse	$\approx 10^9$	≈ 100
Kinetic temperature of particles	≈ 3000 K, cooling somewhat after emission	4–10 K
Particle detector	Windowless electron multiplier	Microchannel plate
Drift-tube temperature	4.2 K	4.2 K
Vacuum	usually $<10^{-12}$ Torr	$<10^{-14}$ Torr

The function of the metal drift tube is to provide electrostatic shielding. However, a charged particle inside the drift tube creates and is attracted to its image charge. For a particle on the axis of a perfect infinitely long cylinder, image-charge forces are balanced by symmetry. The particle is, however, unstable against radial attraction and must be maintained on axis by a longitudinal magnetic field (Sec. III.D).

A cylinder of finite length allows some external field leakage at the ends, reducing the effectively shielded length of the tube from its physical length, H, by about the tube's diameter, $2R$, at either end for $H \gg R$ (Witteborn, 1965).

The drift tube must have a uniform interior diameter, since the charged particle will be attracted by regions of smaller diameter. The electrostatic potential energy of a particle of charge q on the axis of an infinitely long perfect cylinder can be shown to be given by

$$V = -C_1 q^2 / 4\pi\epsilon_0 R , \tag{3.4a}$$

$$C_1 \equiv \int_0^\infty d\omega / \pi I_0^2(\omega) = 0.4353 , \tag{3.4b}$$

where I_0 is the modified Bessel function of zeroth order. If we consider a tapered cylinder with radius R at $z = 0$, increasing to $R + \delta R$ at $z = H$, then the axial force is given by

$$F_z \equiv -dV/dz = -C_1 q^2 \delta R / 4\pi\epsilon_0 R^2 H$$

$$\ll mg , \tag{3.5}$$

which is required to be much smaller than the gravitational force. Thus, for $H = 1$ m and $R = 2$ cm, the uniformity required is of order

$$\delta R \ll \begin{cases} 36 \ \mu\text{m} & \text{(electrons)} \\ 6.5 \text{ cm} & \text{(protons)} \end{cases} , \tag{3.6}$$

both of which are achievable.

The particle may move off axis if the guiding magnetic field is not perfectly aligned with the axis of the drift tube or if the field is not uniform. For an off-axis particle at radial coordinate ρ, the radial force may be shown to be given by

$$F_\rho = C_2(\rho/R) q^2 / 4\pi\epsilon_0 R^2, \quad \rho \ll R , \tag{3.7a}$$

$$C_2 \equiv \int_0^\infty \omega \, d\omega / \pi I_0(\omega) I_1(\omega) = 1.0027 . \tag{3.7b}$$

If we require the work done in displacing the charge from the axis to $\rho = \delta\rho$ to be much smaller than mgH, then, for the previous values of H and R, we require

$$\delta\rho \ll \begin{cases} 0.08 \text{ cm} & \text{(electrons)} \\ 3 \text{ cm} & \text{(protons)} \end{cases} . \tag{3.8}$$

Such alignment of the guide solenoid and its intrinsic magnetic field is easily achieved. However, ambient field variations may cause significant deviations; we examine this in Sec. III.D.

Mutual repulsion limits the linear density of particles

along the drift-tube axis. Witteborn (1965) estimated the electrostatic interaction energy between two particles separated by z_1 on the axis of a long cylinder as

$$\Delta U \approx q^2 e^{-2.4z_1/R} / (0.648) 2\pi\epsilon_0 R \quad (z_1 > R)$$

$$\ll mgH , \tag{3.9}$$

requiring

$$z_1 \gg \begin{cases} 7 \text{ cm} & \text{(electrons)} \\ 0.6 \text{ cm} & \text{(protons)} \end{cases} . \tag{3.10}$$

In the Stanford experiments, low-energy magnetic ground-state electrons were quickly spatially segregated, leaving at most one such electron in the drift tube at a time. In the Los Alamos/CERN experiment, of the 100 or so particles launched, most passed through the drift tube very quickly, again leaving only about one slow particle in the drift tube.

As the charged particle traverses the drift tube, its image charge follows, generating currents within the drift tube. In Sec. VIII we consider the dissipative forces associated with these image-charge currents.

Electric fields inside the drift tube may also arise from the following effects involving the drift tube, which we discuss in later sections:

(a) contact potential patches due to crystal facets and nonuniform contamination (Sec. V),

(b) gravity-induced electric fields: the Schiff-Barnhill effect and the DMRT field (Sec. VI), and

(c) fields induced by thermal gradients (Sec. VII).

C. Electric-field gradients

Electric-field gradients can in principle exert additional forces on polarizable systems. The only significantly polarizable system under consideration is the negative hydrogen ion, for which we give an order-of-magnitude force estimate. We start with the force equation

$$\mathbf{F}_\alpha = \alpha_e \mathbf{E} \cdot \nabla \mathbf{E} . \tag{3.11}$$

We estimate the polarizability α_e by $\alpha_e = (ea_0)^2/\Delta\epsilon$, where a_0 is the Bohr radius of hydrogen, and $\Delta\epsilon$ is the energy required to excite the lowest opposite parity state. Taking $\Delta\epsilon$ as 0.1 eV, we find

$$|F_\alpha / F_g| = 2.74 \times 10^{-13} |\mathbf{E} \cdot \nabla \mathbf{E}| , \tag{3.12}$$

where E is in volts/meter, and ∇E in volts/meter^2. Even with the very large values of $E = 10$ V/m and $\nabla E = 10^3$ V/m^2, we see that $|F_\alpha / F_g| = 3 \times 10^{-9} \ll 1$; hence electric-field-gradient forces are negligible.

D. Magnetic field

For image-charge forces to be negligible, the axial guide magnetic field must maintain the charged particles

sufficiently close to the drift-tube axis, as estimated by $\delta\rho$ in Eq. (3.8). The guide solenoid and its field B can be accurately aligned with the drift-tube axis to angles smaller than $\delta\rho/H$; moreover, solenoids with homogeneities better than about 1 part in 10^5 are commercially available. However, without elaborate magnetic shielding, ambient transverse magnetic-field variations of order $B' \approx 10$ mG can be expected, in which case the net magnetic field may guide the particles sufficiently far off axis for image forces to become significant. Thus B must be large enough that $B'/B \ll \delta\rho/H$, which implies

$$B \gg \begin{cases} 13 \text{ G} & \text{(electrons)} \\ 0.3 \text{ G} & \text{(protons)} \end{cases} \cdot \tag{3.13}$$

In the Stanford experiments, guide fields from 20–40 G were used; in the Los Alamos/CERN experiment, a field of 10–50 kG, much larger than estimated above, is required to reduce the effects of magnetic-field gradients (Sec. III.E).

Charged particles are constrained to move in helixes around the magnetic-field lines, in which they are free to respond to axial forces. Classically, the radius of the helix is given by

$$r = mV_t/eB$$

$$\approx \begin{cases} 28 \text{ nm} & (B = 20 \text{ G}) & \text{(electrons)} \\ 21 \text{ nm} & (B = 50 \text{ kG}) & \text{(protons)} \end{cases}, \tag{3.14}$$

where $V_t \approx 10$ m/s is a typical transverse velocity for slow particles of interest. Thus the charged particles follow the magnetic-field lines very closely by comparison with the scale of typical apparatus.

E. Magnetic-field gradients

Let us assume that **B** is almost parallel to the gravitational field **g**, which defines the z axis of a cylindrical coordinate system. We assume that B has a small gradient in the z direction; i.e., $\mathbf{B} = B_z\hat{z} + B_\rho\hat{\rho}$ with

$|B_z| \gg |B_\rho|$. All the particles of interest possess a magnetic moment μ_z due to their quantized orbital motion in the magnetic field and due to their intrinsic spin, which results in attraction to regions of higher magnetic-field density (paramagnetism). In the H^- ion, the two electron spins are antiparallel, so that its magnetic moment is the same as for a proton; but the electrons are anticorrelated in their orbits, which also results in diamagnetic behavior (Beverini *et al.*, 1986).

1. Paramagnetism

The z-directed force on the particle due to the magnetic-field gradient $\partial B_z/\partial z$ is given by

$$F_z = \mu_z \frac{\partial B_z}{\partial z}, \tag{3.15}$$

where

$$\mu_z = 2\mu_p(n + \tfrac{1}{2} \pm \tfrac{1}{2}\gamma), \quad n = 0, 1, 2, \ldots, \tag{3.16}$$

$$\mu_p = e\hbar/2m \tag{3.17}$$

is the Bohr magneton in the case of electrons, or the nuclear magneton in the case of protons, and

$$\gamma = \begin{cases} 1.001\,159 & \text{(electrons)} \\ 2.792\,844 & \text{(protons)} \end{cases}, \tag{3.18}$$

is due to the spin.

For a group of particles emitted with kinetic temperature T, the average orbital quantum number is given by

$$\bar{n} = kT/\hbar\omega_c, \tag{3.19}$$

where the cyclotron frequency ω_c is given by

$$\omega_c = e|B_z|/m. \tag{3.20}$$

The ratio of the magnetic force to that of gravity is given by

$$|F_z/F_g| = \begin{cases} (2.1 \times 10^6 \text{ m/T})(n + \tfrac{1}{2} \pm \gamma/2)\partial B_z/\partial z & \text{(electrons)} \\ (0.62 \text{ m/T})(n + \tfrac{1}{2} \pm \gamma/2)\partial B_z/\partial z & \text{(protons)} \end{cases} \cdot \tag{3.21}$$

Electrons are emitted with $T \approx 3000$ K, characteristic of the cold cathode (Witteborn and Fairbank, 1977), although some cooling takes place as the electrons interact via Coulomb repulsion. With resistive cooling, antiprotons and H^- ions are expected to be produced with $T = 4$–10 K (Beverini *et al.*, 1986). In all cases, for all practicable sizes of magnetic field, it may be shown that $\bar{n} \gg 1$.

For the majority of emitted electrons then, the condition $|F_z/F_g| \ll 1$ requires an unachievable field uniformity. However, electrons in the magnetic ground state,

where $n = 0$ and the spin is antiparallel, are particularly insensitive since $(n + \tfrac{1}{2} \pm \gamma/2) = 5.8 \times 10^{-4}$, requiring an easily achievable $\partial B_z/\partial z \ll 8$ Gauss/m. In the Stanford experiments, ground-state electrons are spatially segregated from all others by employing a large magnetic-field gradient localized near the emitter (Fig. 1). All non-ground-state electrons are thus quickly accelerated through the system, while the ground-state electrons are slightly decelerated. A disadvantage of this approach is that a large number of launches are required for good statistics, since there is at most one such electron per 10^9

launched.

For protons, the possible values of $(n + \frac{1}{2} \pm \gamma/2)$ would not allow the Stanford technique to be successfully employed. Setting $(n + \frac{1}{2} \pm \gamma/2) \approx \bar{n}$, we have

$$|F_z/F_g| = \frac{kT}{mg} \left| \frac{1}{B_z} \frac{\partial B_z}{\partial z} \right|$$

$$= (842 \text{ m/K})T \left| \frac{1}{B_z} \frac{\partial B_z}{\partial z} \right| . \qquad (3.22)$$

Given that a uniformity of $|(\partial B_z/\partial z)/B_z| \approx 10^{-5}/\text{m}$ is achievable, particularly if a very large field is used to counter ambient field variations, then $T \ll 120$ K is required. This is one of the reasons for cooling the antiprotons and H$^-$ below 10 K. In addition, the distribution of n values produces smearing of the TOF distribution, particularly near cutoff. By using a very large field, $B_z \approx 50$ kG, *and* $T < 10$ K, $\bar{n}$ is decreased and the distribution of n values is more peaked, resulting in less smearing (Beverini *et al.*, 1986).

2. Diamagnetism

The diamagnetic behavior of the H$^-$ ion causes it to be repelled from regions of high magnetic energy density.

This diamagnetism is due mainly to its charge radius. In terms of the diamagnetic polarizability α_m, the diamagnetic force is given by

$$F_z = (\alpha_m/\mu_0)B_z(\partial B_z/\partial z) , \qquad (3.23)$$

where μ_0 is the permeability of free space. The polarizability is given as follows,

$$\alpha_m = -(4\pi/3)a_0^3\alpha^2(r/a_0)^2 , \qquad (3.24)$$

where the root-mean-square radius r is of order a_0, the Bohr radius, and α is the fine-structure constant. Then

$$|F_z/F_g| = (1.6 \times 10^{-3} \text{ m/T}^2)B_z(\partial B_z/\partial z) . \qquad (3.25)$$

This force is negligible in comparison with that due to μ_z for all practicable conditions. Thus H$^-$ ions very closely simulate the electromagnetic properties of antiprotons.

3. Temporal stability

Temporal variations in B_z are less critical. We can estimate the required stability by substituting $\partial B_z/\partial z = (\partial B_z/\partial t)/(dz/dt) < (\partial B_z/\partial t)/v_c$ into Eq. (3.21), where $v_c = (2Hg)^{1/2} = 4.43$ m/s. Even if we set $(n + \frac{1}{2} \pm \gamma/2) \approx \bar{n}$ for both electrons and protons, then Eq. (3.21) yields

$$\frac{1}{|B_z|} \frac{\partial B_z}{\partial t} \ll \begin{cases} 3 \times 10^{-6}/\text{hour} & (T = 3000 \text{ K}) \quad (\text{electrons}) \\ 5/\text{hour} & (T = 4.2 \text{ K}) \quad (\text{protons}) \end{cases} , \qquad (3.26)$$

while the requirement for magnetic ground-state electrons is even less stringent than for protons above. Since superconducting solenoids with a persistence of 10^{-8}/hour are available, we see that the temporal stability of B_z poses no significant problem.

F. Radiation pressure

If S is the radiant power per unit area traveling in a fixed direction, given by Stefan's law, the force it exerts on a particle of radiation cross section σ_r is

$$F_r = (S/c)\sigma_r . \qquad (3.27)$$

For the scattering of photons of energy $\hbar\omega \ll mc^2$ from a free point particle of charge e and mass m, σ_r is given by the Thomson scattering formula (Sakurai, 1967, Secs. 2–5),

$$\sigma_r \approx (8\pi/3)r_c^2 \equiv \sigma_0 , \qquad (3.28)$$

where

$$r_c = e^2/4\pi\varepsilon_0 mc^2 \qquad (3.29)$$

is the classical radius of the particle. While the electron

cross section is much larger than that of the proton, it can be shown that even for room-temperature radiation, F_r is insignificant compared to gravity for both particles.

For the case of radiation scattering from a bound electron in an atomic system, such as the negative hydrogen ion, the cross section is given by the Rayleigh scattering formula modified to include radiation damping (Sakurai, 1967, Secs. 2–6). Specifically,

$$\sigma_r = \sigma_0 \frac{\omega^4}{(\omega_0^2 - \omega^2)^2 + (\gamma\omega)^2} , \qquad (3.30)$$

where σ_0 is the Thomson scattering cross section and $\hbar\omega_0$ is the energy of the lowest excited atomic state coupled to the ground state by a dipole transition. The cross section rises as ω^4 to a peak at $\omega = \omega_0$ with width-at-half-height (due to radiation damping) of $\gamma = (2/3)\omega^2(r_c/c)$.

For the case of thermal radiation at temperature T, with a worst-case solid angle of 2π, we expect a radiation force

$$\mathbf{F}_r = 2\pi \int_0^\pi \sigma_r(\omega) \frac{\hbar\omega^3 d\omega}{(2\pi c)^3(e^{\hbar\omega/kT} - 1)} . \qquad (3.31)$$
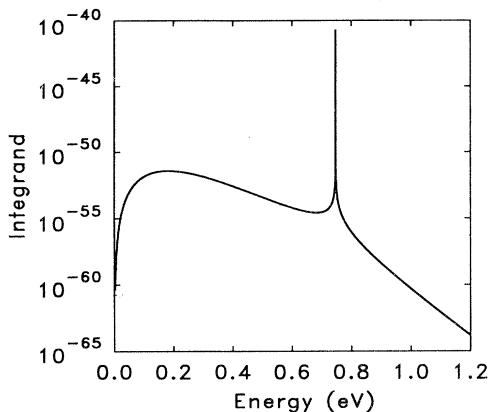
FIG. 5. Integrand in Eq. (3.31) plotted against photon energy.

We illustrate the integrand of this equation in Fig. 5 for the case of the H^- ion with $\hbar\omega_0 = 0.747$ eV (the first electron detachment energy, C. R. C. Handbook, 1980, p. E-67) and $T = 300$ K, whence $\hbar\omega_0 \gg kT$. The integral exhibits a low-energy term F_r' near the peak in the black-body spectrum where the cross section behaves as $(\omega/\omega_0)^4$, and another term F_r'' near the peak in the cross section where the blackbody spectrum is exponentially decreasing:

$$F_r' \approx (\sigma T^4 / c) 16\sigma_0 (\pi kT / \hbar\omega_0)^4$$
$$= (\sigma_0 / c)(2\pi kT^2 / \hbar\omega_0)^4 \sigma \ , \qquad (3.32a)$$

where σ is the Stefan-Boltzmann constant, and

$$F_r'' \approx (2\omega_0^3 \hbar r_c / c^2) e^{-\hbar\omega_0 / kT} \ . \qquad (3.32b)$$

Under these conditions we then find

$$F_r / F_g \approx 2 \times 10^{-8} \ll 1 \ ,$$

and we see that even for thermal radiation pressure at room temperature, this force is negligible.

Another effect involves thermal fluctuations of the electric field inside the drift-tube space, which may lead to diffusion-limited motion for a charged particle. This was investigated by Maris (1974), who found fluctuations to be negligible at 4.2 K for an electron, and even more so for a proton, due to its higher mass (note that an initial mistake by Maris was corrected in a subsequent erratum, Maris, 1974).

IV. RESIDUAL GAS SCATTERING

Collisions with residual gas particles can significantly affect the TOF distribution, requiring operation in ultrahigh vacuum. Cryopumping from 4.2-K walls allowed a vacuum in the drift tube lower than 10^{-12} Torr to be achieved in the WF experiment. For antiparticles, the annihilation rate also limits the tolerable pressure. Beverini *et al.* (1986, p. 96) estimate 10^{-14} Torr is required for antiprotons, which may be achieved with cryo-

pumping and a well-sealed system.

The dominant residual gas expected inside the vacuum space is helium, and we consider its interaction with the beam of charged particles. Some examples of trajectories are shown in Fig. 6. A single upward impulse imparted to a particle [Fig. 6(b)] would decrease its TOF if it would have reached H anyway; and it might increase its TOF beyond $t_c = \sqrt{2H/a}$ if it had already reached its turning point below H [Fig. 6(c)]. Downward impulses cannot increase the TOF beyond t_c unless the particle is subsequently scattered upward to H by a second interaction [Fig. 6(d)].

A point particle of charge q will predominantly interact with a neutral background gas atom by the electrostatic attraction caused by the induced electric dipole moment. This force may be shown to be

$$F = 2\alpha_e q^2 / (4\pi\varepsilon_0)^2 r^5 \ , \qquad (4.1)$$

where $\alpha_e = 2.1 \times 10^{-41}$ fm^2 is the molecular polarizability of helium.

We note that even at 4.2 K, the mean speed V_{He} of the helium atoms will be about 140 m/s, much faster than the speed V_q of the beam particles, which in a typical experiment are expected to be a few m/s. Recall that the guide magnetic field should ensure that only the vertical component of the imparted velocity, ΔV_q, affects the TOF, although the probability of further scatters may be affected by the transverse component.

We therefore assume, after Witteborn, Lockhart, and Fairbank (1988), an impulse approximation for the interaction and estimate the velocity imparted to the virtually stationary particle as a helium atom passes with closest approach distance r_0:

$$\Delta V_q = \frac{3\pi}{8} \frac{1}{mV_{He}r_0^4} \frac{2\alpha_e q^2}{(4\pi\varepsilon_0)^2} \ . \qquad (4.2)$$

The cross section, σ, for the particle to be scattered with a velocity change of *at least* ΔV_q, may be defined as
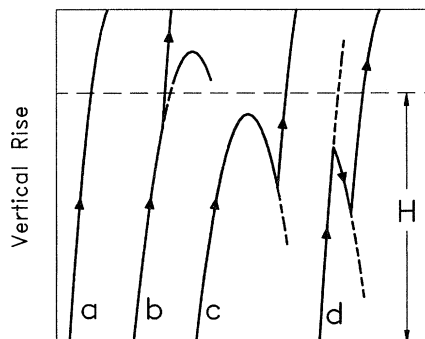

FIG. 6. Effects of gas-atom collisions on the path of a particle projected upwards through the drift tube in a gravitational field, where the time of flight (TOF) to reach height H will be measured: (a) no scatters; the TOF is always less than the cutoff time, t_c; (b), (c), and (d) scatters occur during the flight. Only (c) and (d) can increase the TOF beyond t_c.

$\sigma(\Delta V_q) \equiv \pi r_0^2$. The mean time between such scatters is given by $\tau = 1/n\sigma V_{He}$, where n is the number density of gas atoms given by the ideal-gas formula $P = nkT$, where P is the pressure. Assuming a Maxwellian distribution for the helium atom velocities, $V_{He} = (8kT/\pi M_{He})^{1/2}$, where M_{He} is the mass of a helium atom. The energy imparted by the collision is given by $\Delta E = m(\Delta V_q)^2/2$. Thus τ is given by

$$\tau = (6.0 \times 10^4) T^{3/4} (m\Delta E)^{1/4}/P \quad \text{s} . \tag{4.3}$$

For electrons, $T = 4.2$ K, $P = 10^{-12}$ Torr, and $\Delta E = 10^{-11}$ eV, we find $\tau = 1.5$ s, larger than $t_c = 0.43$ s for $a = g = 9.8$ m/s^2 and $H = 0.91$ m, but a lower pressure would be preferable. Protons are much less sensitive; for the same values of temperature and pressure and $\Delta E = 10^{-9}$ eV (a 1% measurement), we find $\tau \approx 30$ s, and even longer at the vacuum necessary for an acceptable annihilation rate.

If the pressure is high enough that $\tau < t_c$, then there would be significant smearing of the TOF distribution, especially near t_c. We illustrate in Fig. 7 the results of a Monte Carlo computer simulation of gas scattering at various pressures. Note the increased cutoff times at higher pressures and the similarity between the results for $a = g$ and $a = 0$ at $P = 10^{-10}$ Torr.

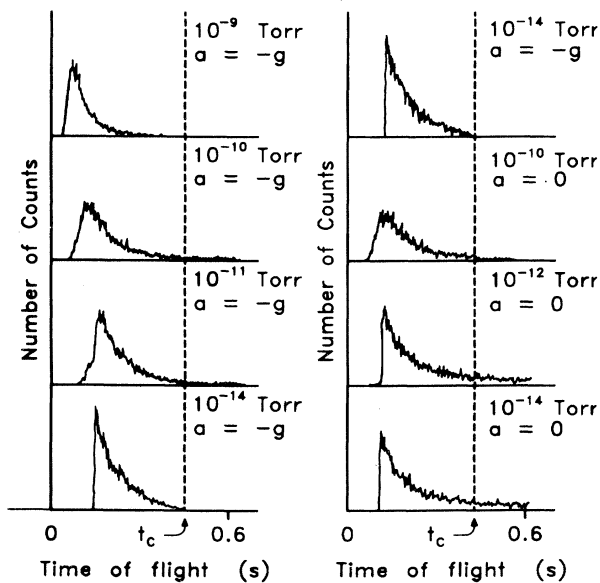An expression may be derived for the minimum detect-

FIG. 7. Monte Carlo simulations of the effects of helium gas scattering on the time-of-flight (TOF) distribution of electrons, for various gas pressures P. $H = 0.9$ m and $T = 4.2$ K. The sharp cutoff at low TOF is due to an upper bound on the initial velocities generated. The dotted line indicates the normal cutoff time $t_c = \sqrt{2H/a}$ when $a = g$. (a) $a = 9.8$ m/s^2, showing the expected clear cutoff at t_c for $P = 10^{-14}$ Torr, but with increased smearing at higher pressures. (b) $a = 0$ (except for top plot where $a = 9.8$ m/s^2 for reference); at 10^{-14} Torr there is no cutoff, as expected.
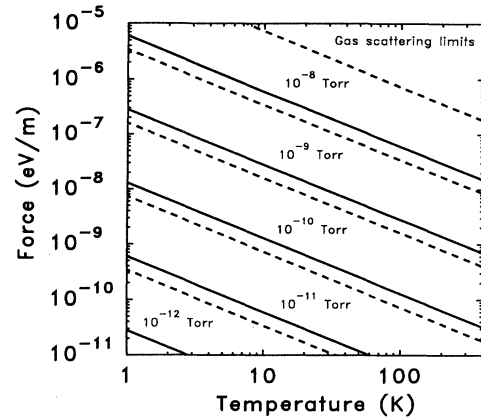
FIG. 8. Minimum detectable uniform ambient force F_{min} as a function of temperature and pressure, due to helium gas scattering in the drift tube. The solid lines apply to electrons, the dashed lines to protons. Forces below the diagonal lines cannot be reliably measured.

able uniform force acting on the charged particle, F_{min}, by setting $\tau = t_c$ and equating the energy imparted by the collision to the work done on the particle by the uniform force over the length of the drift tube. Figure 8 shows this estimated scattering limit as a function of temperature and pressure for electrons and protons; uniform ambient forces well below F_{min} cannot be reliably measured.

V. SURFACE PATCH POTENTIALS

A. Effects on time of flight

Surfaces of metals may exhibit patches of different electric potential due either to the presence of crystal facets of different work functions or to regions with adsorbed surface contaminants, collectively known as the patch effect. We thus expect a spatially random electric potential along the axis of a drift tube. To investigate whether the large number of fluctuations along the tube integrate to cause a significant effect, we consider the energy integral for the time of flight t of a particle of charge q and total energy ε moving vertically in a tube of height H, where at each point the total potential $q\Phi(z) < \varepsilon$:

$$t = \left[\frac{m}{2}\right]^{1/2} \int_0^H dz [\varepsilon - q\Phi(z)]^{-1/2} . \tag{5.1}$$

Expanding the integrand in $[q\Phi(z)/\varepsilon]$, we find

$$t = (m/2\varepsilon)^{1/2} \int_0^H dz \left[1 + \frac{1}{2}\frac{q\Phi(z)}{\varepsilon} + \frac{3}{8}\left[\frac{q\Phi(z)}{\varepsilon}\right]^2 \right.$$
$$\left. + \frac{15}{64}\left[\frac{q\Phi(z)}{\varepsilon}\right]^3 + \cdots \right] . \tag{5.2}$$

The potential may be written as the sum of a smooth potential $\Phi_s(z)$, including that due to gravity, and the ran-

dom potential $\Phi_r(z)$,

$$\Phi(z) = \Phi_s(z) + \Phi_r(z) \ . \tag{5.3}$$

The change of the time of flight due to Φ_r is then

$$\Delta t_r = (m/2\varepsilon)^{1/2} \int_0^H dz \left[\frac{1}{2} \frac{q\Phi_r(z)}{\varepsilon} + \frac{6}{8} \frac{q^2\Phi_s(z)\Phi_r(z)}{\varepsilon^2} \right.$$
$$\left. + \frac{3}{8} \frac{q^2\Phi_r^2(z)}{\varepsilon^2} + \cdots \right] \ . \tag{5.4}$$

The first term in the expansion (5.4) may average to zero over the distance H; however, the even terms will always contribute to the time of flight. In particular, the third term is related to the mean-square potential on axis, $\langle \Phi_r^2 \rangle$. Comparing its contribution, $\Delta t_r'$, with t_c, for the case when gravity is the only force, we require

$$\frac{\Delta t_r'}{t_c} = \frac{3}{16} \frac{e^2 \langle \Phi_r^2 \rangle}{(mgH)^2} \ll 1 \ , \tag{5.5}$$

where $\varepsilon = mgH$ has been used. Thus, for $H = 1$ m, we require

$$\Phi_{\mathrm{RMS}} = \sqrt{\langle \Phi_r^2 \rangle} \ll 0.1 \text{ nV} \quad \text{(electrons)} \ ,$$
$$\ll 0.2 \ \mu\text{V} \quad \text{(protons)} \ . \tag{5.6}$$

B. Estimates of axial potential variations

To calculate the expected value of Φ_{RMS}, we consider a cylinder of infinite length and radius R, which has a potential distribution $\Phi_r(R,\theta,z)$ on its interior surface, which can later be set to zero outside the range $0 < z < H$. The potential on the axis of the cylinder may be shown (Rzchowski and Henderson, 1988; Opat, Moorhead, and Rossi, 1990) to be given by

$$\Phi_r(z) = \int_0^{2\pi} \frac{d\theta'}{2\pi} \int_{-\infty}^{\infty} \frac{dz'}{R} g(z - z') \Phi_r(R,\theta',z') \ , \tag{5.7}$$

where

$$g(z - z') \equiv R \int_{-\infty}^{\infty} \frac{dk}{2\pi} \frac{e^{ik(z-z')}}{I_0(kR)} \ , \tag{5.8}$$

and $I_0(kR)$ is the modified Bessel function of zeroth order (Abramowicz and Stegun, 1965).

Equation (5.7) shows that the axial potential is formed by averaging the surface potential around the tube and convoluting the resulting average with the smoothing function $g(z-z')$. This smoothing function vanishes with exponential rapidity as $|z-z'|/R$ becomes large. Thus surface potentials at points much farther than a radius from the axial point do not contribute to the potential at that point significantly.

After invoking a model (normal Gaussian distribution) for the random surface potential, $\Phi_r(R,\theta,z)$, various authors (Witteborn, 1965; Rzchowski and Henderson, 1988; Opat *et al.*, 1990) have deduced the rms potential on axis to be given by

$$\Phi_{\mathrm{RMS}} = V_0 / \sqrt{N_{\mathrm{eff}}} \ , \tag{5.9}$$

where V_0 is the rms surface potential, and N_{eff} is the effective number of patches contributing to the potential on axis, given by

$$N_{\mathrm{eff}} = (R/w)^2 / C^2 \ , \tag{5.10}$$

where w is a characteristic length scale for patches, which is dependent on the specific model chosen for the patches. The constant C has been calculated as 0.61 (Witteborn), 0.33 (Rzchowski and Henderson), and 0.66 (Opat *et al.*). Thus we may write

$$\Phi_{\mathrm{RMS}} = C \left[\frac{w}{R} \right] V_0 \ , \tag{5.11}$$

showing the attenuation produced when $w \ll R$.

For atomically clean surfaces, the variations between crystal facets are typically $V_0 \approx 0.1$ V. However, oxide layers and other surface contamination generally reduce these to $V_0 \approx 0.01$ V (Darling, 1989). Taking $R = 2$ cm, $V_0 = 0.01$ V, and $C = 0.66$, we find

$$\phi_{\mathrm{RMS}} = \begin{cases} 0.33 \text{ nV} & w = 10 \text{ Å} \\ 0.33 \ \mu\text{V} & w = 1 \ \mu\text{m} \\ 3.3 \text{ mV} & w = 1 \text{ cm} \ . \end{cases} \tag{5.12}$$

Thus experiments with electrons require patch sizes of order atomic dimensions, while those with protons require patch sizes much smaller than 1 μm.

In the Stanford experiments on electrons, crystallites under 1 μm size were visible on the drift-tube surface, which appears to place Φ_{RMS} at odds with their having measured electrons with energies as low as 10^{-11} eV. However, exposure to air would have produced an amorphous surface contaminant layer which appears to mask the underlying crystal structure (Darling, 1989), possibly reducing the patch size to atomic dimensions and possibly also reducing V_0. The temperature-dependent shielding effect claimed by LWF may also be responsible. Various surface coatings and preparation techniques are under investigation by the Los Alamos/CERN group. We stress that it is essential to keep both w and V_0 as small as possible. While surface contamination may mask underlying crystal structure, it also produces small surface-potential variations of order mVs over centimeter length scales, quite unrelated to the underlying structure (Parker and Warren, 1962; Rossi, 1991). Even with $V_0 = 0.1$ mV, for $w = 1$ cm, $\Phi_{\mathrm{RMS}} = 33 \ \mu$V, much too large even for protons.

VI. GRAVITY-INDUCED ELECTRIC FIELD

A. Theory

The gravity-induced electric field *external* to a metallic conductor has been investigated by several authors [Schiff and Barnhill, 1966; Dessler *et al.* (DMRT), 1968;

Herring, 1968; Peshkin, 1968, 1969; Schiff, 1970; Kogan, 1972]. Some of these results were briefly discussed in relation to the Stanford experimental results in Sec. II. Theoretically, the problem consists of adequately describing the surface region of the metal, where the full three-dimensional symmetry of the interior crystal lattice is lost. This problem is compounded when analyzing *real* metal surfaces, which are almost invariably contaminated by oxide layers and other adsorbed species.

As previously noted, the gravity-induced electric field arises because gravity redistributes the electrons and nuclei in a supported metal object. The clearest and most concise formulations of this problem are those of DMRT (1968) and Herring (1968). We review these calculations below and partially extend them in light of a more modern understanding of metal surfaces.

The equilibrium state of the conductor, at constant temperature and volume, can be determined by the condition that the Helmholtz free energy, suitably generalized to include gravitational potential energy, is minimized. The system is then characterized by a *complete chemical potential* of the electrons that is constant throughout the conductor. Here, the complete chemical potential $\bar{\mu}$ is a generalization of the electrochemical potential and includes the gravitational potential energy of the electrons, $m\psi = mgz$, where z is the vertical height. Thus $\bar{\mu}$ is given by

$$\bar{\mu} = \mu - e\phi_{\text{int}} + m\psi , \qquad (6.1)$$

where μ is the ordinary chemical potential (containing kinetic, exchange, and correlation contributions to the electron energy), and $-e\phi_{\text{int}}$ is the internal electrostatic potential energy, averaged over distance scales larger than the screening length but much smaller than the size of the conductor. We take the energy of an isolated electron at rest at infinity to be zero.

The internal electric field can be calculated by taking the gradient of Eq. (6.1) and noting that $\nabla\bar{\mu} = 0$, viz.,

$$\mathbf{E}_{\text{int}} \equiv -\nabla\phi_{\text{int}} = +\frac{m}{e}\mathbf{g} - \frac{1}{e}\nabla\mu . \qquad (6.2)$$

Of particular relevance to the drift-tube experiments is the external electrostatic potential ϕ_{ext}. The calculation of the electrostatic potential is complicated at the surface region of the metal, which extends of order a Fermi wavelength (4.6 Å for copper) on either side of the last ion at the surface (Wigner and Bardeen, 1935; Bardeen, 1936; Herring and Nichols, 1949; Lang and Kohn, 1971). We will show that ϕ_{ext} is related to the work function W of the surface.

Consider two points, $\mathbf{x}_s \pm \hat{\mathbf{n}}\delta$, symmetrically placed about the surface charge at $\mathbf{x}_s$, where $\hat{\mathbf{n}}$ is a unit vector normal to the surface. The distance δ is chosen to be larger than the characteristic depth of the surface region, in particular, sufficiently large that the image potential for an electron at the exterior point is negligible. At the interior point, ϕ_{int} is given by Eq. (6.1). We know from classical electrostatics that the only reason ϕ_{ext}, at the ex-

terior point, differs from ϕ_{int}, at the interior point, is that there is some effective surface dipole-moment density in between which displaces the electrostatic potential on either side, viz.

$$\phi_{\text{ext}}(\mathbf{x}_s + \hat{\mathbf{n}}\delta) - \phi_{\text{int}}(\mathbf{x}_s - \hat{\mathbf{n}}\delta) = \frac{D(\mathbf{x}_s)}{\varepsilon_0} , \qquad (6.3)$$

where D is the normal component of the surface dipole-moment density and ε_0 is the permittivity of free space. Substituting for ϕ_{int} from (6.1), we have

$$-e\phi_{\text{ext}}(\mathbf{x}_s + \hat{\mathbf{n}}\delta) = -m\psi(\mathbf{x}_s - \hat{\mathbf{n}}\delta)$$
$$+ \left[-e\frac{D(\mathbf{x}_s)}{\varepsilon_0} - \mu(\mathbf{x}_s - \hat{\mathbf{n}}\delta) \right] + \bar{\mu} .$$
$$(6.4)$$

For the distance scales chosen above, the bracketed term in (6.4) may be identified as the work function of the metal, viz.,

$$W(\mathbf{x}_s) = -e\frac{D(\mathbf{x}_s)}{\varepsilon_0} - \mu(\mathbf{x}_s - \hat{\mathbf{n}}\delta)$$
$$= \Delta\Phi(\mathbf{x}_s) - \mu(\mathbf{x}_s - \hat{\mathbf{n}}\delta) , \qquad (6.5)$$

where $\Delta\Phi = -eD/\varepsilon_0$ is the energy expended by an electron in going through the dipole layer. This definition of the work function corresponds to the minimum energy required, on average, to remove an electron from the interior to rest just outside the surface region.

The $\mu(\mathbf{x}_s - \hat{\mathbf{n}}\delta)$ component of W reflects the state of the interior of the metal, while $D(\mathbf{x}_s)$ reflects the state of the surface and the result of the evanescent wave functions of electrons tunneling into the vacuum. We note that in addition to gravitational effects, W contains the variation of $D(\mathbf{x}_s)$ over the crystal facets and due to adsorbed dipoles from contamination (the patch effect), as discussed in Sec. V.

From Eqs. (6.4) and (6.5), the external electrostatic potential is given by

$$-e\phi_{\text{ext}}(\mathbf{x}_s + \hat{\mathbf{n}}\delta) = -m\psi(\mathbf{x}_s - \hat{\mathbf{n}}\delta) + W(\mathbf{x}_s) + \bar{\mu} . \qquad (6.6)$$

The determination of the potential in the space external to the conductor requires the value of the potential on the boundary. This potential boundary value is provided by Eq. (6.6). The tangential component of the external electric field, just outside the surface, is immediately given by

$$\hat{\mathbf{t}} \cdot \mathbf{E}_{\text{ext}} \equiv -\hat{\mathbf{t}} \cdot \nabla\phi_{\text{ext}} = \hat{\mathbf{t}} \cdot \left[\frac{m}{e}\mathbf{g} + \frac{1}{e}\nabla W \right] , \qquad (6.7)$$

where $\hat{\mathbf{t}}$ is a unit vector tangent to the surface.

The first term in Eq. (6.2) is the Schiff-Barnhill field, discussed in Sec. II. It reflects the fact that, in the absence of any deformation of the crystal lattice or redistribution of the nuclei, an electric field must be set up by a redistribution of the electrons to balance the force of

gravity on them. The effect is analogous to the acceleration induced emf in electron-inertia experiments (Davis and Opat, 1988; Moorhead, 1991). This field is continued just outside the surface in Eq. (6.7), as is evident from the arguments leading to Eq. (6.3).

Equation (6.7) implies that *whatever else* happens to the distribution of electrons and nuclei under gravity, it must be reflected in a change in the work function. Although we are still left with the difficult task of determining exactly how gravity produces a gradient in the work function, it can nevertheless be determined experimentally. The second term in Eq. (6.7) corresponds to a continuous contact potential variation along the surface and can be investigated by a contact potential measurement that reproduces the effect of gravity on the conductor.

An exact first-principles quantum-mechanical treatment of W would be a formidable task even for an ideal metal surface, let alone one coated with oxide or other contaminants, as was the case in the drift tube used in the Stanford experiments. We can, however, qualitatively describe the physical effects involved.

Firstly, there will be a nonuniform deformation of the metallic lattice calculable by elasticity theory. In such deformation, the mobile conduction electrons will closely follow the distribution of positive ions; otherwise, huge electric fields would result (DMRT, 1968). In turn, this will produce gradients in μ in the interior as a result of the deformation of the primitive cell, with the change in density likely to dominate. Because the internal potentials are altered, the tunneling into the vacuum, and hence D, will change. D is also changed because the deformation changes the areal density of the dipole moments. All of these perturbations will alter $\bar{\mu}$. The mobile conduction electrons will respond, creating a net surface charge whose electric field makes $\bar{\mu}$ constant throughout the system.

Secondly, as gravity shifts the position of the heavier nucleus away from the center of is tightly bound cloud of core electrons, the ion will become polarized, thereby creating an additional electric field. A model including this effect was investigated by Shegelski (1982), who found that this polarization field was canceled by an additional field generated by the conduction electrons. We can understand this simply as a manifestation of the very efficient screening provided by the conduction electrons to any charge perturbation in the system. Thus no net electric field is expected from this effect.

B. Estimates of the fields

As noted in Sec. II, Schiff and Barnhill (1966) deduced only the first term in Eq. (6.7), which places the vertical field at -5.6×10^{-11} V/m. DMRT found in addition the second term in Eq. (6.7) due to the work function, estimating it to be much larger. Herring (1968) pointed out an omission in the Schiff-Barnhill calculation, and it is now generally agreed (Schiff, 1970) that the DMRT calculation is essentially correct.

For a vertically standing drift tube, sufficiently far from the supports, the deformation consists of longitudinal compression that varies linearly with height. Solution of the elasticity equations finally yields

$$u \equiv \sum_i u_{ii} = \frac{\rho g}{3K}(z - H) , \qquad (6.8)$$

$$n \approx n_0(1-u) , \qquad (6.9)$$

where u_{ij} is the strain tensor, u is the dilation, K is the bulk modulus of compressibility, ρ is the mass density, and n_0 and n are the number density of atoms before and after deformation. Assuming that W varies only with dilation, the second term in (6.7) is given by

$$\frac{1}{e}\frac{\partial W}{\partial z} = \gamma \frac{Mg}{e} , \qquad (6.10)$$

where

$$\gamma = \frac{n_0}{3K}\frac{\partial W}{\partial u} \qquad (6.11)$$

and M is the atomic mass. This is the DMRT field, which is proportional to the strain derivative of the work function.

It is convenient to express $\partial W / \partial u$ in terms of the density parameter r_s, the Wigner-Seitz radius,

$$n_e^{-1} = \tfrac{4}{3}\pi r_s^3 , \qquad (6.12)$$

where n_e is the average concentration of conduction electrons. Then

$$\frac{\partial W}{\partial u} = \frac{r_s}{3}\frac{\partial W}{\partial r_s} , \qquad (6.13)$$

and

$$\gamma = \frac{n_0 r_s}{9K}\frac{\partial W}{\partial r_s} . \qquad (6.14)$$

A naive fixed potential-well model of the work function would ignore the changes in D and take μ as the free-electron Fermi kinetic energy, ε_F:

$$\mu \approx \varepsilon_F - \text{constant} ,$$

where

$$\varepsilon_F = \frac{\hbar^2}{2m}\left[\frac{9\pi}{4}\right]^{2/3} r_s^{-2} . \qquad (6.15)$$

Figure 9 shows the density dependence of ε_F. From the above equations we deduce that

$$\gamma \approx \left[\frac{2n_0}{9K}\right]\varepsilon_F . \qquad (6.16)$$

The data for copper (Kittel, 1976) imply $\gamma \approx 0.15$. This would make the DMRT field about 18 000 times larger than the Schiff-Barnhill field.

DMRT considered a more accurate expression for μ from Wigner and Bardeen (1935; Bardeen, 1936) and es-
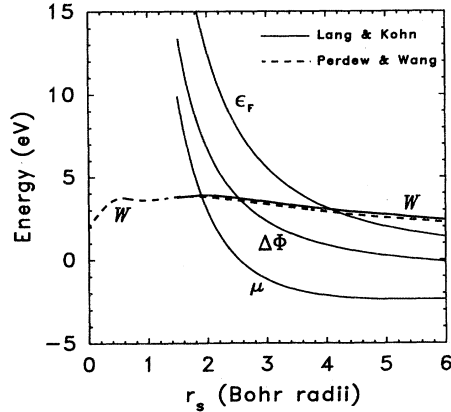
FIG. 9. Density dependence of the work function of jellium and its components. $W = \Delta\Phi - \mu$, where $\Delta\Phi = -eD/\varepsilon_0$. The Wigner-Seitz radius is given by $r_s = (3/4\pi n_e)^{1/3}$, where n_e is the number density of conduction electrons in the bulk, and is usually expressed in units of $a_0 = 0.5$ Å, the Bohr radius. Plotted from the tabulated data of Lang and Kohn (1971), of Lang (in Lundqvist and March, 1983), and of Perdew and Wang (1988).

timated D and its dependence on density from Herring and Nichols (1949). They concluded that this would lower γ from the free-electron estimate but, barring accidental cancellation between D and μ, would still leave a field orders of magnitude larger than the Schiff-Barnhill field.

In fact, modern density-functional theory, using the jellium model for a metal surface, predicts that γ may be much smaller. Heine and Hodges (1972) have discussed the physical reasons for there being a large degree of cancellation between the components of W, $\Delta\Phi$, and μ in Eq. (6.5). If μ increases, raising the internal electron levels closer to the vacuum, the electrons tunnel further out, making D more negative. Thus $\Delta\Phi$ increases and compensates for μ. This is evident in Fig. 9, taken from the calculations of Lang and Kohn (1971) for W and its components, including the high-density results of Perdew and Wang (1988). While $\Delta\Phi$ and μ vary considerably, W is relatively insensitive to density. These calculations predict that $\partial W/\partial r_s$, and hence γ, is zero for certain densities $[(r_s/a_0) \approx 0.6, 1.0, 1.8$, where $a_0 = 0.53$ Å is the Bohr radius], in which case the DMRT field is zero. For copper $(r_s/a_0) = 2.67$ and $\partial W/\partial(r_s/a_0) \approx -0.44$ eV. Thus $\gamma \approx -0.013$, an order of magnitude smaller and of *opposite* sign to the previous estimate. This still leaves the DMRT field about 1500 times larger than the Schiff-Barnhill field and so should dominate over the force of gravity in drift-tube experiments with electrons. For antiprotons it would be slightly smaller.

The density-functional/jellium calculations have had great success in predicting the properties of simple metals. For the transition and noble metals it is not expected to be as accurate; e.g., the predicted work function for copper is about 20% lower than experimentally measured values for polycrystalline samples. Models including the crystal lattice reduce this discrepancy; e.g., the

nine-atom slab calculation of Smith *et al.* (1980) predicts the work function of the (100) face of copper crystals within 3%. However, these refined calculations represent only single numerical results for specific crystal planes which, unfortunately, do not yield much insight regarding the density dependence of the work function. At present it appears that the jellium results are the only useful guidance we have for predicting the DMRT field.

If the crystallinity of the metal is considered, we may expect that the work function also depends on deformation without a change in density, i.e., shear strain, particularly the surface dipole moment. However, we note that the relevant surface for the drift tubes is the contaminant surface layer rather than the underlying bulk metal. In the case of the Stanford drift tube, the complex chemistry (Sec. II) would make this surface nearly amorphous, in which case jellium may be a reasonable model, although the density parameter may not be the same as for the underlying metal. Experiments conducted in our group (Rossi, 1991) on similar copper surfaces yield values close to the jellium predictions for $\partial W/\partial r_s$ (this will be the subject of a future paper).

At present, it must be admitted that the theoretical understanding of real metal surfaces cannot accurately predict the value of the DMRT field. While the problem may be tackled experimentally, measurements conducted on one surface may not apply to the drift-tube surface due to the sensitivity to variations in surface contamination. One way to approach this difficulty would be to include a mechanism in the free-fall apparatus for differentially straining the drift tube along its axis, i.e., in addition to that due to gravity. In this way the DMRT field could be studied *in situ*. The Los Alamos/CERN experiments may shed further light on whether or not the DMRT field is really shielded as proposed by the Stanford group.

VII. THERMOELECTRIC FIELD

A temperature gradient in a conductor will produce an additional external electric field. To find this additional field we generalize Eq. (6.6) to include the temperature dependence of the work function and of the complete chemical potential:

$$-e\phi_{\text{ext}}(\mathbf{x}_s + \hat{\mathbf{n}}\delta) = -m\psi(\mathbf{x}_s - \hat{\mathbf{n}}\delta) + W(\mathbf{x}_s, T) + \bar{\mu}(T) ,$$

$$(7.1)$$

where T is the temperature. Differentiating this equation gives the external electric field. The result for the gravity-induced field, in the previous section, followed from the fact that $\nabla\bar{\mu} = 0$ in an isothermal conductor carrying no electric current. When T varies, this is no longer true; in this case, $\nabla\bar{\mu}$ must be derived from the appropriate phenomenological equations.

Davis and Opat (1988) have discussed heat and electric current flow in a nonisothermal conductor subject to gravity and strain, obtaining the following familiar pair of equations:

$$I = \frac{\sigma}{e} \nabla \bar{\mu} - \sigma S \nabla T , \tag{7.2}$$

$$J = \frac{\sigma}{e} S T \nabla \bar{\mu} - (\kappa + \sigma S^2 T) \nabla T , \tag{7.3}$$

where **I** is the electric current density, **J** is the heat current density, σ is the electrical conductivity, κ is the thermal conductivity, S is the Seebeck coefficient (or absolute thermoelectric power), and $\bar{\mu}$ has been generalized to the complete chemical potential used above. If no electric current is allowed to flow in the conductor, then only Eq. (7.2) is required and we have

$$\nabla \bar{\mu} = e S \nabla T . \tag{7.4}$$

For a vertically standing drift tube with a temperature gradient along its axis and no electric current, Eqs. (7.1) and (7.2) give the external electric field just outside the surface as

$$E_z = \left[\frac{-mg}{e} + \frac{1}{e} \frac{\partial W}{\partial z} \right] + E_T , \tag{7.5}$$

where the first two terms are the gravity-induced field derived previously, and E_T, the thermoelectric field, is given by

$$E_T = \left[\frac{1}{e} \frac{\partial W}{\partial T} + S \right] \frac{dT}{dz} ,$$

$$= \bar{S} \frac{dT}{dz} , \tag{7.6}$$

where $\bar{S}$ is a generalized thermoelectric coefficient that includes the temperature dependence of the work function. This gives the thermoelectric field in terms of two experimentally measurable quantities, $\partial W / \partial T$ and S.

For metals, S is of order 1 μV/K at room temperature; semiconductors exhibit much larger values of order 1 mV/K; superconductors, in contrast, have $S = 0$. At low temperatures, thermodynamics predicts that $S \rightarrow 0$ as $T \rightarrow 0$. Gold *et al.* (1960) have measured the thermoelectric power of Cu below 20 K, finding values as small as 0.05 μV/K, although impure samples exhibited anomalous values as high as 16 μV/K.

The temperature dependence of the work function is less well known. Gartland *et al.* (see the review by Hölzl and Schulte, 1979) find 10–20 μV/K for Cu monocrystals at 300 K. In contrast, Lee *et al.* (1969) find a value of about 1 mV/K for cesiated tungsten surfaces at 300 K. As in the case of S, it is expected that $\partial W / \partial T \rightarrow 0$ as $T \rightarrow 0$ (Herring and Nichols, 1949). Data for semiconductors seem scarce, but probably $(1/e)(\partial W / \partial T) \approx S$. Shott and Walton (1977) have measured the temperature dependence of the work function of superconducting tin below the critical temperature, finding the surprisingly large value of 2 mV/K.

The temperature-gradient-induced electrostatic force on a charged particle of mass m and charge e compared to gravity is given by

$$eE_T / F_g = \frac{e\bar{S}}{mg} \frac{dT}{dz}$$

$$= \begin{cases} 1.8 \times 10^4 \ dT/dz & \text{(electrons)} \\ 9.8 \ dT/dz & \text{(protons)} \end{cases} , \tag{7.7}$$

assuming $\bar{S} \sim 1 \ \mu$V/K. Thus we require

$$\frac{dT}{dz} \ll \begin{cases} 6 \times 10^{-5} \ \text{K/m} & \text{(electrons)} \\ 0.1 \ \text{K/m} & \text{(protons)} \end{cases} . \tag{7.8}$$

Temperature gradients below 10^{-5} K/m may be achieved with care by limiting heat dissipation and connecting the drift tube at one point only with a good thermal shunt to the liquid-helium bath (Witteborn and Fairbank, 1977).

It might be thought that a semiconducting oxide surface layer on a drift tube (i.e., CuO and/or Cu_2O on Cu) would exhibit larger thermoelectric fields, since $S \sim 1$ mV/K instead of 1 μV/K for most metals. However, in this case, there will be thermoelectric currents flowing along the oxide layer and back into the metal substrate. In a simplified model with a thin oxide layer on an infinite metal substrate and a fixed temperature gradient along the junction, Eq. (7.1) gives

$$\frac{\partial \bar{\mu}_{\text{oxide}}}{\partial z} = \left[\frac{e}{\sigma_{\text{oxide}}} \right] I_{z,\text{oxide}} + (e S_{\text{oxide}}) \frac{dT}{dz} , \tag{7.9}$$

where

$$I_{z,\text{oxide}} = \sigma_{\text{oxide}} (S_{\text{metal}} - S_{\text{oxide}}) \frac{dT}{dz} . \tag{7.10}$$

The resulting equation for E_T is

$$E_T = \left[\frac{1}{e} \frac{\partial W_{\text{oxide}}}{\partial T} + S_{\text{metal}} \right] \frac{dT}{dz} . \tag{7.11}$$

This calculation would have to be modified at 4.2 K, where most semiconductors behave essentially as insulators, since the carriers are frozen out. It may then be shown that the external tangential field E_T is still given by (7.11). In any case, if the work function of the oxide layer had an anomalously high temperature dependence, say of order 1 mV/K, then a severe limit would be placed on permissible temperature gradients in experiments with electrons or positrons.

The work function of a surface may be strongly temperature dependent due to adsorption of dipoles from a background gas. A temperature gradient along the surface will produce a gradient in the amount of adsorbed species and also in the work function. De Waele *et al.* (1973) found the temperature dependence for Cu to be normally around -10 μV/K at 4.2 K. However, the presence of sufficient He gas to cover the sample with a monolayer produces a very strong temperature dependence near 4.2 K of about 3 mV/K. This levels off, to the value it had before admission of He, at about 8 K (see
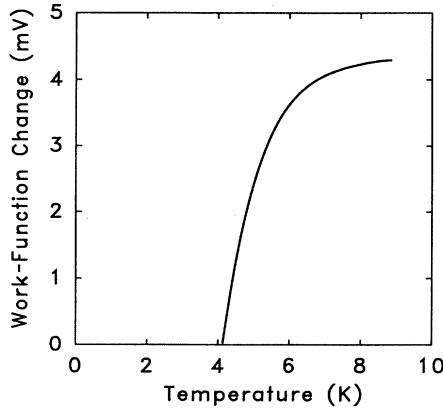
FIG. 10. Temperature dependence of the work function of copper due to an adsorbed monolayer of helium. Reproduced from the data published by de Waele *et al.* (1973).

Fig. 10). They interpret this as strong desorption of He above 4.2 K.

We would expect a drift tube with adsorbed gases and a temperature gradient to show a strongly temperature-dependent electric field due to such desorption phenomena as were observed by de Waele *et al.* This would provide a natural explanation for the temperature-dependent force observed by LWF, if there was more adsorbed gas on their drift tube than was originally supposed.

VIII. IMAGE CURRENT DISSIPATION

A group of particles of total charge Q outside a conductor creates an image charge $-Q$ on its surface. When this group of particles moves in any direction (normal or parallel to the surface), the image charge follows in an appropriate way. It may be shown that this redistribution of surface charge $-Q$ is accomplished by the flow of electric currents in the bulk (not surface) of the conductor. Such currents dissipate energy ohmically, and as a consequence, the particle group experiences an effective frictional force. Under certain circumstances such a frictional force can heavily damp the motion of the group. We investigate this problem.

The equations controlling the flow of charge in an isothermal conductor are

$$\mathbf{I} = \sigma \mathbf{E}, \quad \text{Ohm's law} , \tag{8.1}$$

$$\nabla \cdot \mathbf{E} = 0, \quad \text{electrical neutrality of conductor} . \tag{8.2}$$

The conductivity is denoted by $\sigma = 1/\rho$, where ρ is the resistivity.

The results of solving the boundary-value problem implied by Eq. (8.1) and (8.2) using Fourier techniques yield for the power dissipated

$$P = Q^2 \rho (V_p^2 + 2V_n^2)/(16\pi Z^3) , \tag{8.3a}$$

where Z is the distance of the charge group from the surface (see also Boyer, 1974), and V_p and V_n are the veloci-

ties of the group, parallel and normal to the surface, respectively.

A second case we wish to consider is a surface that has a resistive slab of thickness b on a resistanceless substrate. Then the power dissipated may be shown to be

$$P = 3bQ^2 \rho (V_p^2 + 2V_n^2)/(32\pi Z^4) . \tag{8.3b}$$

We may define a dissipation time τ for motion parallel to the surface as

$$\tau \equiv -V_p/(dV_p/dt) .$$

For the cases above we find

$$\tau = 16\pi Z^3 M/Q^2 \rho , \tag{8.4a}$$

$$\tau = 32\pi Z^4 M/3bQ^2 \rho . \tag{8.4b}$$

In the first case, estimating the resistivity of the drift tube to be of order $\rho = 10^{-9}$ Ωm at 4.2 K for copper, (Witteborn and Fairbank, 1977; a higher value may be expected for the antiproton drift tube, depending on the surface coating used), for a group of N particles of charge e, and $Z = 2$ cm, Eq. (8.4a) yields

$$\tau \approx \begin{cases} 1 \times 10^{13}/N & \text{(sec) (electrons)} \\ 3 \times 10^{16}/N & \text{(sec) (protons)} \end{cases} . \tag{8.5a}$$

The Stanford apparatus launches of order 10^9 electrons, but only one or less is expected with a TOF near $t_c \approx 0.45$ s. The Los Alamos CERN apparatus is expected to launch about 100 particles, but again only about one slow particle is expected. Even if all the particles launched were present together in a group, for this case, damping is expected to be quite negligible in both experiments.

In the second case, we have in mind a semiconducting surface film on the bulk metal of the drift tube, e.g., copper oxide on copper for the Stanford drift tube. The resistivity of Cu_2O is about 10^8 Ωm at 293 K (Herrmann and Wagener, 1951, p. 128). If the carriers in such a semiconducting surface layer were not frozen out at 4.2 K, retaining a similar resistivity, for a thickness of $b = 100$ Å, we estimate

$$\tau \approx \begin{cases} 200/N & \text{(sec) (electrons)} \\ 4 \times 10^5/N & \text{(sec) (protons)} \end{cases} . \tag{8.5b}$$

Since $N \leq 1$, for slow particles near cutoff, damping is expected to be negligible for both experiments even in this extreme second case.

We note that if severe damping were present, the particles would reach a terminal velocity V_{term} soon after entering the drift tube. This would show up clearly in the TOF distribution as a peak around H/V_{term} with a marked lowering of the count rate for short TOFs, instead of the usually observed smooth inverse power-law decay with a cutoff. The same applies to any other dissipative forces, such as extreme gas scattering (Sec. IV), and to forces that produce diffusive motion, such as thermal fluctuations in the electric field (Sec. III.F).

IX. SUMMARY

We have exhaustively listed and studied the various influences on the motion of a charged particle under gravity in a drift-tube apparatus. The great importance of such experiments, testing the weak equivalence principle for antimatter, requires that these influences be carefully studied. By use of the clever techniques developed by the Stanford and Los Alamos/CERN groups, most spurious interactions can be rendered negligible. However, uncertainty remains over electric fields produced by the patch effect and gravitationally induced strain gradients in the drift tube (the DMRT field). While the temperature-dependent shielding effect claimed by the Stanford group may be genuine, it has not been independently verified, despite various attempts to do so. The preliminary experiments by the Los Alamos/CERN group with H$^-$ and heavier ions may shed more light on this issue. A great advantage of the antiproton experiment is that only a differential measurement against H$^-$ is proposed. We anticipate exciting results that may be forthcoming in the near future.

ACKNOWLEDGMENTS

APPENDIX: SUPPLEMENTARY BIBLIOGRAPHY

The following literature survey is a supplement to the references quoted in the main text. While no claims can be made for completeness, it includes most of the other published and unpublished work known to us on drift-tube experiments, gravity-induced electric fields, and related topics.

A. Effect of gravity, acceleration, and strain on matter

1. Theoretical

Anandan, J., 1981, "Gravitational and inertial effects in quantum fluids," Phys. Rev. Lett. **47**, 463.

Anandan, J., 1984a, "Relativistic thermoelectromagnetic gravitational effects in normal conductors and superconductors," Phys. Lett. A **105**, 280.

Anandan, J., 1984b, "Effect of Newtonian gravitational potential on a superfluid Josephson interferometer," Phys. Rev. B **30**, 3717.

Balakin, A. B., and J. G. Ignat'ev, 1983, "The effect of a gravitational wave at the contact of conductors," Phys. Lett. A **96**, 10.

Barnett, S. J., 1935, "Gyromagnetic and electron-inertia effects," Rev. Mod. Phys. **7**, 129.

Barnhill, M. V., 1968, "Rotation-induced electric fields near metals," Phys. Lett. A **27**, 461.

Blackford, B. L., M. G. Calkin, A. J. Purcell, and G. Siroink, 1979, "Rotation induced electromotive forces in normal and superconducting metals," Can. J. Phys. **57**, 39.

Cerdonio, M., and S. Vitale, 1984, "Superfluid He4 analog of the rf superconducting quantum interference device and the detection of inertial and gravitational fields," Phys. Rev. B **29**, 481.

Chow, R., and W. A. Tiller, 1984, "Deformation-induced work function changes in Cu single crystals. II. Theory," J. Appl. Phys. **55**, 1346.

Darwin, C. G., 1936, "The inertia of electrons in metals," Proc. R. Soc. London, Ser. A **154**, 61.

DeWitt, B. S., 1966, "Superconductors and gravitational drag," Phys. Rev. Lett. **16**, 1092.

Ginzburg, V. L., and S. M. Kogan, 1972, "Electron-inertial experiments," Sov. Phys. JETP **34**, 628.

Gron, O., and K. Voyenli, 1982, "Charge distributions in rotating conductors," Eur. J. Phys. **3**, 210.

Harrison, W. A., 1969, "Force on an electron near a metal in a gravitational field," Phys. Rev. **180**, 1606.

Held, A., 1967, "The behaviour of free electrons and positrons within a closed metallic container," Nuovo Cimento A **63**, 976.

Houston, W. V., 1940, "Acceleration of electrons in a crystal lattice," Phys. Rev. **57**, 184.

Hunter, S. C., and F. R. N. Nabarro, 1953, "The propagation of electrons in a strained metallic lattice," Proc. R. Soc. London, Ser. A **220**, 542.

Lang, I. G., and S. T. Pavlov, 1970, "Microscopic theory of the Stewart-Tolman effect," Sov. Phys. Solid State **12**, 836.

Lang, I. G., and S. T. Pavlov, 1971, "Deformation-potential interaction between conduction electrons and ultrasonic waves," Sov. Phys. Solid State **12**, 1926.

Leontovich, M. A., and V. T. Khait, 1971, "Possibility of experimentally measuring the electromagnetic field produced in a metal in which transverse ultrasonic waves propagate," JETP Lett. **13**, 414.

Leung, M. C., 1972, "Electric fields induced by gravitational fields in metals," Nuovo Cimento B **7**, 220.

Leung, M. C., G. Papini, and R. G. Rystephanick, 1971, "Gravity-induced electric fields in metals," Can. J. Phys. **49**, 2754.

Michel, F. C., 1968, "On the measurement of differences between the gravitationally induced electric fields near various metals," Phys. Rev. Lett. **21**, 104.

Nieto, M. M., and T. Goldman, 1980, "Measurement of G/h using the superconducting AC Josephson effect," Phys. Lett. A **79**, 449.

Papini, G., 1966, "London moment of rotating superconductors and Lense-Thirring fields of general relativity," Nuovo Cimento B **65**, 66.

Papini, G., 1969, "Gravity-induced electric fields in superconductors," Nuovo Cimento B **63**, 549.

Rieger, T. J., 1970, "Gravitationally induced electric field in metals," Phys. Rev. B **2**, 825.

Rostoker, N., 1952, "Interpretation of the electron-inertia experiments for metals with positive Hall coefficients," Phys. Rev. **88**, 952.

Schrader, R., 1984, "On the electromagnetic response to gravitational waves," Phys. Lett. B **143**, 421.

Shockley, W., 1952, "Interpretation of e/m values for electrons in crystals," Phys. Rev. **88**, 953.

Strnad, J., 1971, "The gravity-induced electric field," Contemp. Phys. **12**, 187.

Tannhauser, D. S., 1968, "Concerning an experiment to measure the difference between gravitationally induced electric field near various metals," Phys. Rev. Lett. **20**, 1123.

Tsidil'kovskii, I. M., 1975, "Electrons and holes in an inertial-force field," Sov. Phys. Usp. **18**, 161.

2. Experimental

Andreev, L. A., and Ya. Palige, 1964, "Change of the electron work function of molybdenum and tantalum upon cold deformation under ultrahigh vacuum conditions," Sov. Phys. Dok. **8**, 1003.

Beams, J. W., 1968, "Potentials on rotor surfaces," Phys. Rev. Lett. **21**, 1093.

Brown, C. R., J. B. Brown, E. Enga, and M. R. Halse, 1971, "Contact potential changes produced by very small stresses," J. Phys. D **4**, 298.

Brown, S., and S. J. Barnett, 1952, "Carriers of electricity in metals exhibiting positive Hall coefficients," Phys. Rev. **87**, 601.

Chow, R., and W. A. Tiller, 1984, "Deformation-induced work function changes in Cu single crystals I. Experiment," J. Appl. Phys. **55**, 1339.

Craig, P. P., 1969, "Direct obervations of stress-induced shifts in contact potentials," Phys. Rev. Lett. **22**, 700.

Craig, P. P., and V. Radeka, 1970, "Stress dependence of contact potential: the AC Kelvin method," Rev. Sci. Instrum. **41**, 258.

Enga, E., 1974, "Strain induced potentials on a 'dirty' polycrystalline surface," Can. J. Phys. **52**, 708.

French, S. H., and J. W. Beams, 1970, "Contact-potential changes produced on metal surfaces by tensile stresses," Phys. Rev. B **1**, 3300.

Gerbshtein, Yu. M., E. I. Nikulin, and F. A. Chudnovskii, 1983, "Pressure-induced emf in a metal-superionic-metal system," Sov. Phys. Solid State **25**, 659.

Goldstein, Y., M. Cohen, and B. Abeles, 1970, "Strain-induced electric fields in superconducting aluminum," Phys. Rev. Lett. **25**, 1571.

Guptill, E. W., 1971, "Electric field near an accelerating copper tube," Can. J. Phys. **49**, 3150.

Hendricks, J. B., C. A. King, and H. E. Rorschach, 1971, "Magnetization by rotation: the Barnett effect in a superconductor," J. Low Temp. Phys. **4**, 209.

Kettering, C. F., and G. G. Scott, 1944, "Inertia of the carrier of electricity in copper and aluminum," Phys. Rev. **66**, 257.

Kompan, M. E., 1983, "Gravity-induced emf in superionic conductor RbAg$_4$I$_5$," JETP Lett. **37**, 327.

Leners, K. H., R. J. Kearney, and M. J. Dresser, 1972, "Stress-dependent contact potential in copper," Phys. Rev. B **6**, 2943.

Mints, R. I., V. P. Melekhin, and M. B. Partenskii, 1975, "Deformation-induced change in the work function of electrons," Sov. Phy. Solid State **16**, 2330.

Rzchowski, M. S., and W. M. Fairbank, 1984, "Spatial resolution of low temperature surface potentials," in *Proceedings of the 17th International Conference on Low Temperature Physics*, edited by U. Eckern, A. Schmid, W. Weber, and H. Wühl (Elsevier, Amsterdam), p. 1361.

Schumacher, J. C., W. E. Spicer, and W. A. Tiller, 1972, "Strain dependence of Cu work function," talk at annual meeting of the American Physical Society, 31 January–3 February 1972, San Francisco.

Scott, G. G., 1951, "Inertia of the carrier of electricity in cad-mium," Phys. Rev. **83**, 656.

Tinder, R. F., 1968, "Stress dependence of ion and thermionic emission," J. Appl. Phys. **39**, 355.

Tolman, R. C., S. Karrer, and E. W. Guernsey, 1923, "Further experiments on the mass of the electric carrier in metals," Phys. Rev. **21**, 525.

Tolman, R. C., and L. M. Mott-Smith, 1926, "A further study of the inertia of the electric carrier in copper," Phys. Rev. **28**, 794.

Tolman, R. C., and T. D. Stewart, 1916, "The electromotive force produced by the acceleration of metals," Phys. Rev. **8**, 97.

Tolman, R. C., and T. D. Stewart, 1917, "The mass of the electric carrier in copper, silver and aluminum," Phys. Rev. **9**, 164.

Witteborn, F. C., and M. R. Pallesen, 1967, "Experimental upper limit to differences between the gravitationally induced electric fields near various metals," Phys. Rev. Lett. **19**, 1123.

B. Drift-tube experiments and other studies of gravity

1. Theoretical

Beverini, N., L. Bracci, and G. Torelli, 1986, "Stochastic cooling of charged particles in a Penning trap," Europhys. Lett. **1**, 435.

Darling, T. W., and G. I. Opat, 1987, "A possible explanation for rapid changes in the time-of-flight distribution in the Witteborn-Fairbank experiment" (University of Melbourne), Report No. UM-P-87/45.

Gillies, G. T., 1990, "Resource Letter MNG-1: Measurements of Newtonian gravitation," Am. J. Phys. **58**, 525.

Gron, O., and E. Eriksen, 1989, "Translational inertial dragging," Gen. Relativ. Gravit. **21**, 105.

Jain, A. K., J. E. Lukens, and J. S. Tsai, 1987, "Test for relativistic gravitational effect on charged particles," Phys. Rev. Lett. **58**, 1165.

Lesche, B., 1989, "A test of the principle of equivalence for the second generation," Gen. Relativ. Gravit. **21**, 623.

Matz, D., and F. A. Faempffer, 1958, "Some considerations on the gravitational mass of antimatter," Bull. Am. Phys. Soc. Ser. II **3**, 317.

Schrader, R., 1984, "On the electromagnetic response to gravitational waves," Phys. Lett. B **143**, 421.

Silverman, M. P., 1987, "Gravitationally induced quantum interference effects on fermion antibunching," Phys. Lett. A **122**, 226.

Torelli, G., and N. Beverini, 1986, "Antiproton traps and related experiments," in *Nuclear and Particle Physics at Intermediate Energies with Hadrons*, edited by T. Bressani and G. Pauli (Societa Italiana di Fisica, Bologna).

Worden, P. W., Jr., and C. W. F. Everitt, 1982, "Resource Letter GI-1: Gravity and Inertia," Am. J. Phys. **50**, 494.

2. Experimental

Brown, R. E., 1986, "Proposed measurement of the gravitational acceleration of the antiproton," LANL Report LA-UR-86-1806.

Levin, D. S., 1986, "A Low Temperature Search for Surface Charge Anomalies on Oxidized Copper," M.Sc. thesis (San Francisco State University).

Lockhart, J. M., 1976, "Experimental Evidence for a Temperature-Dependent Surface Shielding Effect inside a Copper Tube," Ph.D. thesis (Stanford University).

Lockhart, J. M., F. C. Witteborn, and W. M. Fairbank, 1975,

"Observation of a temperature-dependent shielding effect inside a copper tube," in *Proceedings of the 14th International Conference on Low Temperature Physics,* edited by M. Krusius and M. Vuorio (Elsevier, New York), p. 274.

Opat, G. I., J. V. Hajnal, and S. J. Wark, 1988, "Gravitational experiments with beams of particles of non-zero rest mass," in *Proceedings of the 5th Marcel Grossmann Meeting on General Relativity,* edited by D. G. Blair and M. J. Buckingham (World Scientific, Singapore), p. 1583.

Pipes, P. B., and D. H. Darling, 1975, "Temperature dependence of contact potential in superconducting niobium," in *Proceedings of the 14th International Conference on Low Temperature Physics,* edited by M. Krusius and M. Vuorio (Elsevier, New York), p. 571.

Rigby, K. W., 1986, "Surface Cyclotron Resonance and Anomalies in the Surface Impedance of Metals at Low Temperatures," Ph.D. thesis (Stanford University).

Rigby, K. W., and W. M. Fairbank, 1984, "Anomalies in the microwave surface impedance of copper and aluminium," in *Proceedings of the 17th International Conference on Low Temperature Physics,* edited by U. Eckern, A. Schmid, W. Weber, and H. Wühl (Elsevier, Amsterdam), p. 1363.

Witteborn, F. C., and W. M. Fairbank, 1968, "Experiments to determine the force of gravity on single electrons and positrons," Nature **220,** 436.

Witteborn, F. C., L. V. Knight, and W. M. Fairbank, 1965, "Use of low-temperature techniques to measure gravitational forces on charged particles," in *Proceedings of the 9th International Conference on Low Temperature Physics,* edited by J. G. Daunt, D. O. Edwards, F. J. Milford, and M. Yaqub (Plenum, New York), p. 1248.

REFERENCES

Abramowicz, M., and I. A. Stegun, 1965, Eds., *Handbook of Mathematical Functions* (Dover, New York).

Adelberger, E. G., S. W. Stubbs, B. R. Heckel, Y. Su, H. E. Swanson, G. Smith, J. H. Gundlach, and W. F. Rogers, 1990, Phys. Rev. D **42,** 3267.

Ashcroft, N. W., and N. D. Mermin, 1976, *Solid State Physics* (Holt, Rinehart, and Winston, New York).

Bardeen, J., 1936, Phys. Rev. **49,** 653.

Bardeen, J., 1982, talk for "Near Zero Conference," Stanford, March 25, 1982, published in *Near Zero: New Frontiers in Physics,* edited by C. W. F. Everitt (Freeman, San Francisco, 1987).

Beverini, N., J. H. Billen, B. E. Bonner, L. Bracci, R. E. Brown, L. J. Campbell, D. A. Church, K. R. Crandall, D. J. Ernst, A. L. Ford, T. Goldman, D. B. Holtkamp, M. H. Holzscheiter, S. D. Howe, R. J. Hughes, M. V. Hynes, N. Jarmie, R. A. Kenefick, N. S. P. King, V. Lagomarsino, G. Manuzio, M. M. Nieto, A. Picklesimer, R. M. Thaler, G. Torelli, T. P. Wangler, M. Weiss, and F. C. Witteborn, 1986, CERN Proposals CERN/PSCC/86-2, PSCC/P94 and CERN/PSCC/86-26, PSCC/M260, and LANL Report No. LA-UR-86-260.

Bondi, H., 1957, Rev. Mod. Phys. **29,** 423.

Boyer, T. H., 1974, Phys. Rev. A **9,** 68.

Boynton, P. E., D. Crosby, P. Ekstrom, and A. Szumilo, 1987, Phys. Rev. Lett. **59,** 1385.

Braginsky, V. B., and V. I. Panov, 1971, Sov. Phys. JETP **34,** 464.

Brown, R. E., J. B. Camp, and T. W. Darling, 1990, in *Application of accelerators in research and industry,* Proceedings of the 11th International Conference, Denton, Texas, 5–8 November, 1990, edited by H. H. Anderson and S. T. Picraux (Nucl. Instrum. Methods Phys. Res., Sec. B, **56/57,** Part 1, p. 480).

Cabrera, N., and N. F. Mott, 1949, Rep. Prog. Phys. **12,** 163.

Camp, J. B., T. W. Darling, and R. E. Brown, 1991, J. Appl. Phys. **69,** 7126.

Darling, T. W., 1989, "Electric fields on metal surfaces at low temperatures," Ph.D. thesis (University of Melbourne, Australia).

Davis, T. J., 1987, "Electromagnetic effects of accelerated matter," Ph.D. thesis (University of Melbourne, Australia).

Davis, T. J., and G. I. Opat, 1988, Class. Quantum Grav. **5,** 1011.

Delchar, T. A., 1971, Surf. Sci. **27,** 11.

Dessler, A. J., F. C. Michel, H. E. Rorschach, and G. T. Trammell, 1968, Phys. Rev. **168,** 737.

de Waele, A. Th. A. M., R. De Bruyn Ouboter, and P. B. Pipes, 1973, Physica (Utrecht) **65,** 587.

Eckhardt, D. H., C. Jekeli, A. R. Lazarewicz, and A. J. Romaides, 1988, Phys. Rev. Lett. **60,** 2567.

Fairbank, W. M., F. C. Witteborn, J. M. J. Madey, and J. M. Lockhart, 1974, in *Experimental Gravitation,* edited by B. Bertotti (Academic, New York), p. 310.

Fischbach, E., D. Sudarsky, A. Szafer, C. Talmadge, and S. H. Aronson, 1986, Phys. Rev. Lett. **56,** 3.

Free, J. U., C. D. Dermer, and P. B. Pipes, 1979, Phys. Rev. B **19,** 631.

Gold, A. V., D. K. C. MacDonald, and W. B. Pearson, 1960, Philos. Mag. **5,** 765.

Goldman, T., R. J. Hughes, and M. M. Nieto, 1986, Phys. Lett. B **171,** 217.

Goldman, T., R. J. Hughes, and M. M. Nieto, 1987, Phys. Rev. D **36,** 1254.

Goldman, T., and M. M. Nieto, 1982, Phys. Lett. B **112,** 437.

Good, M. L., 1961, Phys. Rev. **121,** 311.

Hanni, R. S., and J. M. Madey, 1978, Phys. Rev. B **17,** 1976.

Heine, V., and C. H. Hodges, 1972, J. Phys. C **5,** 225.

Henderson, J. R., and W. M. Fairbank, 1984, in *Proceedings of the 17th International Conference on Low Temperature Physics* (LT-17, Part II), Universität Karlsruhe and Kernforschungszentrum Karlsruhe, August, 1984, edited by U. Eckern, A. Schmid, W. Weber, and H. Wühl (Elsevier, Amsterdam), p. 1359.

Herrmann, G., and S. Wagener, 1951, *The Oxide-Coated Cathode,* Vol. II (Chapman and Hall, London).

Herring, C., 1968, Phys. Rev. **171,** 1361.

Herring, C., and M. H. Nichols, 1949, Rev. Mod. Phys. **21,** 185.

Hölzl, J., and F. K. Schulte, 1979, in *Solid Surface Physics,* Springer Tracts in Modern Physics Vol. 85, edited by G. Höhler (Springer-Verlag, Berlin), p. 1.

Hutson, A. R., 1978, Phys. Rev. B **17,** 1934.

Jackson, J. D., 1975, *Classical Electrodynamics,* 2nd ed. (Wiley, New York).

Kittel, C., 1976, *Introduction to Solid State Physics,* 5th ed. (Wiley, New York).

Kogan, Sh. M., 1972, Sov. Phys. Usp. **14,** 658.

Kolb, E. W., and M. S. Turner, 1983, Annu. Rev. Nucl. Part. Sci. **33,** 645.

Lang, N. D., and W. Kohn, 1971, Phys. Rev. B **3,** 1215.

Lee, T. J., B. J. Hopkins, and B. H. Blott, 1969, J. Appl. Phys. **40,** 3825.

Lockhart, J. M., 1976 "Experimental evidence for a temperature-dependent surface shielding effect inside a copper

tube," Ph.D. thesis (Stanford University).

Lockhart, J. M., F. C. Witteborn, and W. M. Fairbank, 1977, Phys. Rev. Lett. **38**, 1220.

Lockhart, J. M., F. C. Witteborn and W. M. Fairbank, 1991, Phys. Rev. Lett. **67**, 283.

Lundqvist, S., and N. H. March, 1983, *Theory of the Inhomogeneous Electron Gas* (Plenum, New York).

Macrae, K. I., and R. J. Riegert, 1984, Nucl. Phys. B **244**, 513.

Maris, H. J., 1974, Phys. Rev. Lett. **33**, 1177; **33**, 1594(E).

Moorhead, G. F., 1991, "Acceleration induced electromotive force," Ph.D. thesis (University of Melbourne, Australia).

Morrison, P., 1958, Am. J. Phys. **26**, 358.

Morrison, P., and T. Gold, 1957, *Essays on Gravity* (Gravity Research Foundation, New Boston, NH).

Nieto, M. M., and T. Goldman, 1991, Phys. Rep. **205**, 221.

Nieto, M. M., T. Goldman, and R. J. Hughes, 1988, Phys. Rev. D **38**, 2937.

Ohanian, H. C., 1977, Am. J. Phys. **45**, 903.

Opat, G. I., G. F. Moorhead, and F. Rossi, 1990, University of Melbourne Report UM-P-90/62.

Parker, J. H., and R. W. Warren, 1962, Rev. Sci. Instrum. **33**, 948.

Perdew, J. P., and Y. Wang, 1988, Phys. Rev. B **38**, 12228.

Peshkin, M., 1968, Ann. Phys. (N.Y.) **46**, 1.

Peshkin, M., 1969, Phys. Lett. A **29**, 181.

Roll, P. G., R. Krotkov, and R. H. Dicke, 1964, Ann. Phys. (N.Y.) **26**, 442.

Rose, B. A., 1933, Phys. Rev. **44**, 585.

Rossi, F., 1991, "Gravity and strain induced potentials in metals," Ph.D. thesis (University of Melbourne, Australia).

Rzchowski, M. S., and J. R. Henderson, 1988, Phys. Rev. A **38**, 4622,

Rzchowski, M. S., K. W. Rigby, and W. M. Fairbank, 1987,

Jpn. J. Appl. Phys. **26**, Suppl. 26-3, 651.

Sakurai, J. J., 1967, *Advanced Quantum Mechanics* (Addison-Wesley, New York).

Scherk, J., 1979, Phys. Lett. B **88**, 265.

Schiff, L. I., 1958, Phys. Rev. Lett. **1**, 254.

Schiff, L. I., 1970, Phys. Rev. B **1**, 4649.

Schiff, L. I., and M. V. Barnhill, 1966, Phys. Rev. **151**, 1067.

Shegelski, M. R. A., 1982, "A simple model for studying the gravitationally induced electric field inside a metal," M.Sc. thesis (University of British Columbia).

Shott, M., and A. J. Walton, 1977, Phys. Lett. A **60**, 63.

Smith, J. R., J. G. Gay, and F. J. Arlinghaus, 1980, Phys. Rev. B **21**, 2201.

Stacey, F. D., G. J. Tuck, G. I. Moore, S. C. Holding, B. D. Goodwin, and R. Zhou, 1987, Rev. Mod. Phys. **59**, 157.

Thieberger, P., 1987, Phys. Rev. Lett. **58**, 1066.

Trammell, G. T., and H. E. Rorschach, 1970, Phys. Rev. B **2**, 4761.

von Eötvös, R., D. Pekar, and E. Fekete, 1922, Ann. Phys. (Leipzig) **68**, 11.

Weast, R. C., 1980, Ed., *C.R.C. Handbook of Physics and Chemistry*, 60th ed. (Chemical Rubber, Boca Raton).

Wigner, E., and J. Bardeen, 1935, Phys. Rev. **48**, 84.

Will, C. M., 1984, Phys. Rep. **113**, 345.

Witteborn, F. C., 1965, "Free fall experiments with negative ions and electrons," Ph.D. thesis (Stanford University).

Witteborn, F. C., and W. M. Fairbank, 1967, Phys. Rev. Lett. **19**, 1049.

Witteborn, F. C., and W. M. Fairbank, 1977, Rev. Sci. Instrum. **48**, 1.

Witteborn, F. C., J. M. Lockhart, and W. M. Fairbank, 1988, private communication.